175

EFFECT OF SUBSTITUTION OF DEUTERIUM FOR HYDROGEN IN WATER ON THE ELECTROCHEMICAL KINETICS OF STAINLESS STEEL-304

159

by

SHIV NATH KAUL

B. S. (Chem. Engg.) BANARAS HINDU UNIVERSITY, INDIA, 1957

A MASTER'S THESIS

submitted in partial fulfillment of the

requirements for the degree

MASTER OF SCIENCE

Department of Nuclear Engineering

KANSAS STATE UNIVERSITY
Manhattan, Kansas

1965

Approved by:

S. Z. Mikhail

Major Professor

CONTENTS

LIST OF TABLES

LIST OF FIGURES

NOMENCLATURE

A	Morse constant
A_1, A_2	Constants
B	Eyring's entropy function
C	Concentration
$D°$	Bond dissociation energy
E_o	Total energy based on zero
E_{corr}	Corrosion potential
E_L	Liquid junction potential
F	Faraday
$F°$	Total partition function for the activated state
G	Free energy
I	Ionization potential
K	Equilibrium constant
K_F	Force constant in Hook's law
M	Metal electrode
N	Avogadro's number
Q	Partition function
R	Gas constant
R	Ratio of exchange current densities
S	Separation factor
T	Temperature
U_+, U_-	Mobilities
V_M	Irreversible potential difference at the metal solution boundary
X	Contact potential difference between metals

X^*	Activated complex
Z, Z_+, Z_-	Valencies
a_H	Activity of the adsorbed hydrogen on the surface in gm atoms per cm^2
a_{H^+}	Activity of the hydrogen ions on the electrode surface
b	Tafel slope
d	Dielectric constant of medium
e	Unit charge
h	Planck's constant
i	Current density amps/cm^2
i_c	Current density amps/cm^2 at cathode
i_o	Exchange current density, amps/cm^2
k	Boltzmann constant
k'	Specific rate of reaction
r	Effective radius
r	Ratio of H to HD rates
s	Entropy
t_+, t_-	Transference numbers
v_1	Direct reaction rate
v_2	Reverse reaction rate
ΔG	Gibbs free-energy change
ΔG_s	Free energy of solvation
ΔH_s	Heat of solvation
ΔH^*	Standard heat of activation
χ	Fraction of the surface covered with adsorbed H_2

α	Fraction of the electrical potential operative between the initial and the activated states
β	Symmetry factor
ϕ_M	Work function of the metal M
η	Overvoltage
λ	Number of electrons necessary for one act of rate determining step
π_f	The product of partition functions of H and D containing reactants
τ	Transmission coefficient
μ	Stoichiometric number
μ_m	Reduced mass
ν	Frequency
ζ	Zeta potential
θ	Surface coverage
Θ	Confidence limits
ε	Electronic charge
$\varepsilon_0, \varepsilon_1, \varepsilon_2$	Energy of single molecule in the various possible levels

1.0 INTRODUCTION

Stainless steel type 304, because of its good mechanical properties and corrosion resistance, is often used as structural and cladding material in nuclear reactors (1, 2). In most reactors the surface of stainless steel, either of cladding or of structural material, is in contact with water or heavy water used as coolant or moderator (3). It is, therefore, imperative to study the behavior of stainless steel-304 in these two environments from the viewpoint of surface reactions and corrosion resistance.

Since corrosion processes are most often electrochemical (4), the electrokinetic study on a particular surface leads to a clear conception of the mechanism of corrosion. Today it can be considered as an established fact that the primary cause of corrosion is the thermodynamic instability of most metals and alloys in atmospheric conditions and in water solutions. The ultimate aim of corrosion studies is to investigate methods of controlling corrosion by limiting the surface reactions either by changing the environmental condition or by changing the composition of the material.

Many researchers have studied such problems by electrochemical measurements on pure substances (5, 6, 7). Work on alloys by such methods, on the other hand, is lagging. In the case of stainless steel, e.g., most of the studies have been directed towards passivity (8, 9, 10).

The purpose of this thesis was to study the electrokinetics of a freshly electropolished surface of stainless steel-304 in water and heavy water and to find the effect of deuterium substitution on the kinetics and mechanism of reactions. This work leads to the determination of a value for the electrolytic separation factor, S, defined as the ratio of the concentration of hydrogen to deuterium in the gas phase to the corresponding ratio in the solution phase in an electrolytic separation cell. Such a factor is of extreme importance in heavy water preparation by the process of electrolytic separation, which process has received and is still receiving utmost care in the production of heavy water. From knowledge of the separation factor and the standard heats of activation of the rate determining steps in water and heavy water, further insight into the reaction mechanism was obtained.

2.0 THEORETICAL DEVELOPMENT

2.1 Electrode Potential and Overvoltage

In a complete galvanic cell consisting of an electrode of metal M and a Pt electrode in the same solution, there are three potential differences:

1) V_M, that at the metal-solution boundary

2) V_{Pt}, at the Pt- solution boundary

and 3) X, the contact potential difference between M and Pt.

If ΔV_e is the equilibrium potential difference measured by means of a potentiometer connected to wires of composition M, then

$$\Delta V_e = V_{Me} - V_{Pte} + X \tag{1}$$

where subscript e denotes equilibrium potentials. Now $X = \phi_M - \phi_{Pt}$ where ϕ_M and ϕ_{Pt} are the work functions of the metals M and Pt respectively. Hence

$$\Delta V_e = V_{Me} - V_{Pte} + \phi_M - \phi_{Pt} \ . \tag{2}$$

If, in the cell considered above, the cathode carries a current density i, a different potential difference will arise given by

$$\Delta V = V_M - V_{Pt} + \phi_M - \phi_{Pt} \tag{3}$$

where ΔV = irreversible potential difference between the metal cathode and the Pt electrode

and V_M = irreversible potential difference at the metal solution boundary.

$V_{Pt} = V_{Pte}$ if the platinum electrode is used as a reference hydrogen electrode which is the case in all overpotential measurements.

$\Delta V - \Delta V_e$ is denoted by η, the overvoltage. Or

$$\Delta V = \Delta V_e + \eta \ . \tag{4}$$

Writing Eq. (3) in terms of the overvoltage and equilibrium potential, it follows that

$$\Delta V_e + \eta = V_M - V_{Pt} + \phi_M - \phi_{Pt} \tag{5}$$

$$V_M = \Delta V_e + \eta + V_{Pt} - \phi_M + \phi_{Pt} \ . \tag{6}$$

In the cell considered above, if the Pt electrode acts as a hydrogen electrode, then for a given pH and temperature ΔV_e, V_{Pt}, ϕ_{Pt} are constant. Therefore, Eq. (6) can be written as

$$V_M = \eta - \phi_M + K' \tag{7}$$

where
$$K' = \Delta V_e + V_{Pt} + \phi_{Pt}. \tag{8}$$

The relation between the Cathodic current density i_c and the potential V_M, for a kinetic electrode process in which the reverse reaction can be neglected, is given (11) by an equation of the form (see below)

$$i_c = k_1 \exp(-\alpha V_M F/RT) \tag{9}$$

where α and k_1 are constants, F is faraday, R is gas constant, and T is absolute temperature.

Thus by substituting from Eq. (6)

$$i_c = k_1 \exp(-\alpha(\eta - \phi_M + K')F/RT) \tag{10}$$

if $i_c = i_o$, when $\eta = 0$, then

$$i_o = k_2 \exp(\alpha\phi_M F/RT) \tag{11}$$

and Eq. (10) can be written then in terms of i_o as

$$i_c = i_o \exp(-\alpha\eta F/RT) \tag{12}$$

i_o, known as the exchange current, is characteristic of the particular electrode used and is taken as a basis for comparison of various electrodes in overvoltage studies. Eq. (12) can also be derived from the theory of absolute reaction rates as follows.

In order for any chemical change to take place, it is necessary for the atoms or molecules involved to come together to form an activated complex.

This is illustrated by the equation

$$A + B \rightleftarrows X^* \rightleftarrows C + D \tag{13}$$

where X^* is the activated complex. This complex is regarded as being situated at the top of an energy barrier lying between the initial and final stages, and the rate of the reaction is controlled by the rate with which the complex travels over the top of the barrier.

According to the theory of absolute reaction rates (12) the specific rate k' of any reaction is given by the expression

$$k' = \tau(kT/h)\exp(-\Delta F/RT) \tag{14}$$

where τ is a constant introduced to allow for the possibility that not every activated complex reaching the top of the potential energy barrier is converted into reaction products, and is called the transmission coefficient. (Except for limited cases, τ is usually taken as unity.)

For a reversible electrode the specific rate of the discharge process, i.e., of the direct reaction, may, therefore, be written as

$$k_1' = (kT/h)\exp(-\Delta G_1^*/RT) \tag{15}$$

while for the reverse reaction

$$k_2' = (kT/h)\exp(-\Delta G_2^*/RT) \tag{16}$$

the equilibrium constant $K = k_1'/k_2' = \exp(-(\Delta G_1^* - \Delta G_2^*)/RT)$ (17)

where ΔG_1^* = standard free energy of activation for the direct reaction

and ΔG_2^* = standard free energy of activation for the reverse reaction.

At the reversible potential, where Eqs. (15) and (16) hold good, no current passes, but if an overvoltage, η, is applied, the rate of the direct reaction exceeds that of the reverse process and current flows at a definite rate. Without making any assumptions as to the mechanism of the discharge process, it may be supposed that the effect of the excess potential is to diminish the free energy increase requisite for the formation of the activated state from reactants, thus assisting the direct process, whereas the reverse process is retarded. If the additional potential, η, acts across the energy barrier between initial and final states, and α is the fraction of this electrical potential operative between the initial and activated states (α has a most probable value of 0.5 for the discharge reaction as determined experimentally (12)), then the potential, $\alpha\eta$, will facilitate the formation of the latter by decreasing the free energy by an amount $\alpha\eta F$. (See figure 1)

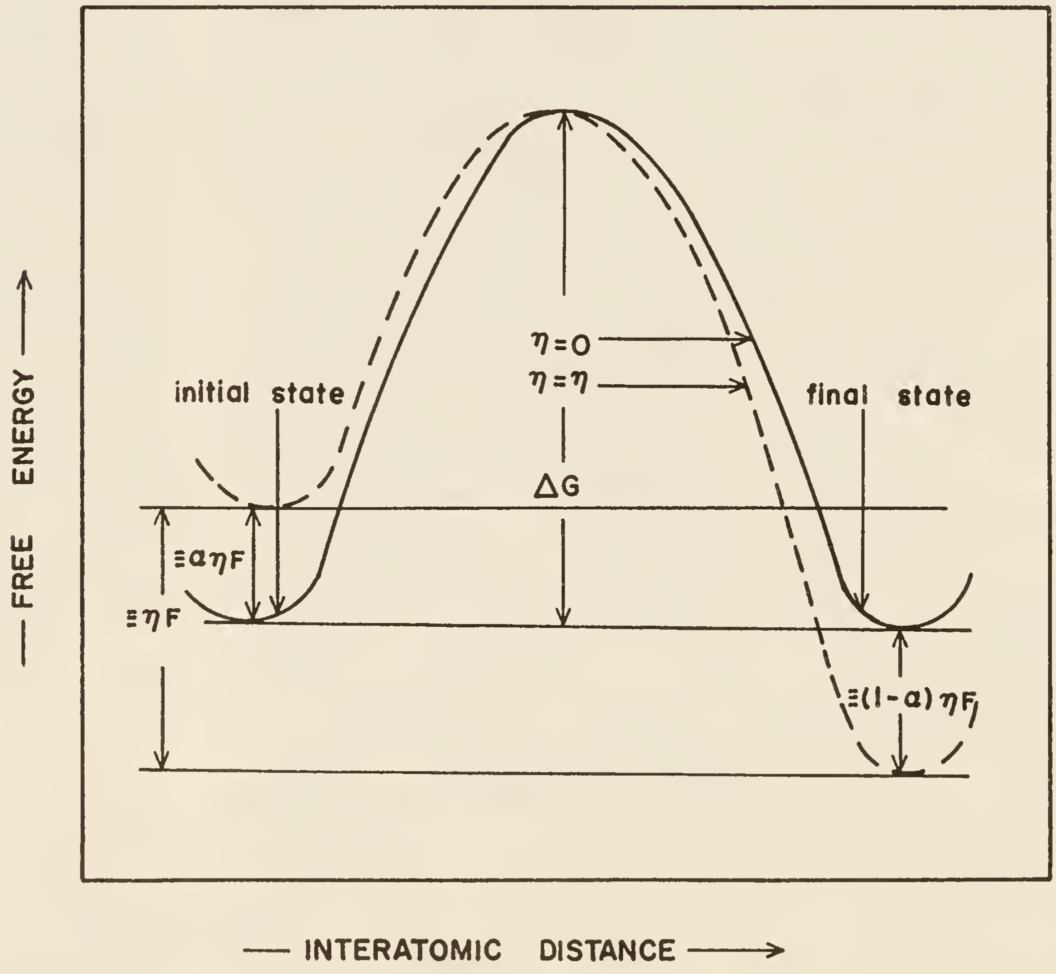

Fig. 1. Energy Barrier Diagram

At the same time the potential will oppose the reverse reaction, increasing the free energy required by $(1 - \alpha)\eta F$. The specific rates for direct and reverse reactions at the overvoltage, η, are then

$$k_1' = (kT/h)\exp(-\Delta G_1^*/RT)\exp(-\alpha\eta F/RT) \tag{18}$$

and

$$k_2' = (kT/h)\exp(-\Delta G_2^*/RT)\exp((1 - \alpha)\eta F/RT) \tag{19}$$

or

$$k_1' = A_1 \exp(-\alpha\eta F/RT) \tag{20}$$

and

$$k_2' = A_2 \exp((1 - \alpha)\eta F/RT) \tag{21}$$

where A_1 and A_2 are constants. Since no assumptions have been made concerning the nature of the reactants and resultants, their concentrations may be represented by C_1 and C_2 units, i.e., atoms, molecules or ions, per square cm of the electrode surface so that the direct and reverse reaction rates, in units per square cm, related to the specific reaction rate constants

$$v_1 = k_1'C_1$$

$$v_2 = k_2'C_2$$

$$v_1 = A_1C_1 \exp(-\alpha\eta F/RT) \tag{22}$$

and

$$v_2 = A_2C_2 \exp((1 - \alpha)\eta F/RT) \ . \tag{23}$$

The current passing is determined by the difference between these rates, and if each reacting unit may be regarded as carrying the equivalent of a single charge, the current density i, in amp. per sq. cm, is given by

$$i = (v_1 - v_2)F/N$$

$$= (C_1A_1 \exp(-\alpha\eta F/RT) - C_2A_2 \exp((1 - \alpha)\eta F/RT)F/N \tag{24}$$

where F is the faraday, i.e., 96,500 coulombs and N is Avogadro's number. If η is small, i.e., for very low overvoltages, the exponentials may be expanded and all terms other than the linear ones neglected. Thus

$$i_c = [C_1A_1(1 - \alpha\eta F/RT) - C_2A_2(1 + (1 - \alpha)\eta F/RT)]F/N \ . \tag{25}$$

It is seen from Eq. (25) that at the reversible potential, where $\eta = 0$ and $i_c = 0$, $C_1A_1 = C_2A_2$. If this equality may be assumed to hold also for small values of η, Eq. (25) becomes

$$i_c = (C_1A_1\eta F/RT)F/N \ . \tag{26}$$

At low overvoltages, therefore, there should be a linear relationship between current and overvoltage. This has been found to be true for the evolution of hydrogen and the deposition of metals (12). For higher values of η, the rate of the reverse reaction becomes negligibly small in comparison with that of the discharge process so that it is possible to write

$$i_c = (C_1A_1 \exp(-\alpha\eta F/RT))F/N = i_o \exp(-\alpha\eta F/RT) \ . \tag{27}$$

Current, i_o, the significance of which has been indicated above is equal to C_1A_1F/N. The factor, α, in Eq. (27) can be considered as the product of two factors, β and λ (11), where λ equals the number of electrons necessary so that one act of the rate determining step can occur and β is the symmetry factor. Eq. (27) can, therefore, be written in the form

$$i_c = i_o \exp(-\beta\lambda\eta F/RT) \tag{28}$$

or

$$\eta = (RT/\beta\lambda F)\ln i_o - (RT/\beta\lambda F)\ln i_c \ . \tag{29}$$

Eq. (29) can be written in the form

$$\eta = a - b \ln i_c \tag{30}$$

where

$$a = (RT/\beta\lambda F)\ln i_o \tag{31}$$

and

$$b = RT/\beta\lambda F = -d\eta/d\ln i_c \ . \tag{32}$$

Eq. (30) is usually called Tafel equation and "b" called Tafel slope. By definition, β and λ values are given by

$$o<\beta<1 \quad \text{and} \quad \lambda = 1 \text{ or } 2. \tag{33}$$

2.2 Kinetics of the Hydrogen Evolution Reaction

It has been shown (11) that the possible reaction paths of the hydrogen evolution reaction in acid solutions are mainly

$$\left.\begin{array}{ll} H_3O^+ + e + M \xrightarrow{\text{Slow}} MH_{ads} + H_2O & \text{I} \\ MH_{ads} + MH_{ads} \xrightarrow{\text{Fast}} 2M + H_2 & \text{II} \end{array}\right\} \quad \text{(A)}$$

$$\left.\begin{array}{ll} H_3O^+ + e + M \xrightarrow{\text{Fast}} MH_{ads} + H_2O & \text{III} \\ MH_{ads} + MH_{ads} \xrightarrow{\text{Slow}} 2M + H_2 & \text{IV} \end{array}\right\} \quad \text{(B)}$$

$$\left.\begin{array}{ll} H_3O^+ + e + M \xrightarrow{\text{Slow}} MH_{ads} + H_2O & \text{V} \\ H_3O^+ + MH_{ads} + e \xrightarrow{\text{Fast}} H_2 + H_2O & \text{VI} \end{array}\right\} \quad \text{(C)}$$

and

$$\left.\begin{array}{ll} H_3O^+ + e + M \xrightarrow{\text{Fast}} MH_{ads} + H_2O & \text{VII} \\ H_3O^+ + MH_{ads} + e \xrightarrow{\text{Slow}} H_2 + H_2O & \text{VIII} \end{array}\right\} \quad \text{(D)}$$

Additional possible reaction courses are given in reference (11).

The slow reactions I, IV and VIII are rate determining steps and are commonly termed simple discharge, atomic desorption and electrochemical desorption mechanisms of the electrolytic evolution of hydrogen, respectively.

Each of the reaction paths A, B, C, and D is discussed below:

(I) Reaction Paths A and B

The source of the protons is H_3O^+ and the atomic hydrogen reaction is desorptive.

General Kinetic Equations

The reactions and velocities v_1 and v_2 to be considered are

$$H_3O^+ + e + M \xrightarrow{v_1} MH_{ads} + H_2O \tag{34}$$

$$MH_{ads} + H_2O \xrightarrow{v_2} H_3O^+ + e + M \quad (35)$$

and
$$MH_{ads} + MH_{ads} \xrightarrow{v_3} H_2 + 2M \quad (36)$$

The velocity of the reverse desorption reaction of Eq. (36) is assumed to be negligible at potentials greater than the reversible hydrogen potential.

The potential difference between the cathode and the solution represented by ΔV_c consists of two parts. These two parts are ΔVp, between the cathode and the plane passing through the center of ions adjacent to the cathode surface and ζ, between this plane and the bulk of the solution. This is based on the concept of the existence of an electrical double layer, at the electrode solution boundary (13), consisting of two oppositely charged layers of ions at a fixed distance apart. This double layer is regarded as equivalent to an electrical condenser of constant capacity with parallel plates separated by a distance of the order of a molecular diameter.

From the theory of absolute reaction rates discussed above, the specific rate constant of reaction (34) is given by

$$k_1' = (kT/h)\exp[-(\Delta F + \alpha\Delta VpF)/RT] \quad (37)$$

where ΔF is the free energy change of reaction (34) when $\Delta Vp = 0$, but since the reaction rate $v_1 = a_1 k_1'$ where the activity of the hydrogen ions on the electrode surface $a_1 = a_{H^+}(1 - \chi)$, a_{H^+} being the activity of hydrogen ions in the electrical double layer and χ being the fraction of electrode surface covered with adsorbed hydrogen. Therefore, from Eq. (37)

$$v_1 = k_1 a_{H^+}(1 - \chi)\exp(-\Delta VpF/2RT) \ . \quad (38)$$

If there are 10^{15} free spaces for adsorption per cm^2 of the electrode surface and χ is the fraction of the surface covered with adsorbed hydrogen atoms, then the number of atoms of hydrogen adsorbed per $cm^2 = \chi.10^{15}$. Since 1 atom of hydrogen is approximately 10^{-24} gm atom, then activity a_H of the adsorbed hydrogen in gm atoms per $cm^2 = \chi\ 10^{-9}$. Hence for reaction (35), the rate v_2 can be expressed as

$$v_2 \doteq k_2 10^{-9} \chi \exp(\Delta VpF/2RT) \tag{39}$$

and for reaction (36)

$$v_3 = k_3 10^{-18} \chi^2 \ . \tag{40}$$

In the steady state

$$v_1 - v_2 - 2v_3 = 0 \ . \tag{41}$$

Solving Eqs. (38), (39), (40) and (41) for χ gives the real solution

$$\chi = \frac{-(A_1 + A_2) + \sqrt{(A_1 + A_2)^2 + 8A_1A_3}}{4A_3} \tag{42}$$

where $$A_1 = k_1 a_{H^+} \exp(-\Delta VpF/2RT) \tag{43}$$

$$A_2 = 10^{-9} k_2 \exp(\Delta VpF/2RT) \tag{44}$$

and $$A_3 = 10^{-18} k_3 \ . \tag{45}$$

For reactions (34), (35) and (36), the net current at steady state is, therefore

$$i_c = \lambda F(v_1 - v_2) = 2\lambda F v_3 = 2Fv_3 \tag{46}$$

and from Eqs. (40), (42) and (46)

$$i_c = 2F10^{-18} k_3 \chi^2 = 2FA_3 \chi^2 \tag{47}$$

$$= (F/8A_3)[-(A_1 + A_2) + ((A_1 + A_2)^2 + 8A_1A_3)^{1/2}]^2 \ . \tag{48}$$

(I-1) Simple Discharge is Rate Determining (Path A)

(i) General condition

$$(v_1 + v_2) \ll v_3 \tag{49}$$

since $v_1 \propto A_1$

and $v_2 \propto A_2$

therefore, $(A_1 + A_2) << A_3$

or $10(A_1 + A_2) < A_3$ (50)

where factor 10 is selected as an arbitrary limit of significance (11). The linking of v_1 and v_2 or A_1 and A_2 by a positive sign in the condition is clear, since, by the nature of the reactions concerned, a decrease in A_2 increases χ, thereby decreasing A_1 and increasing A_3; that is, a decrease in A_2 increases the probability of the slow discharge mechanism.

(ii) Coverage of surface

The velocity v_1 is much greater than v_2 to allow the slow discharge reaction to proceed in the forward direction, then

$$A_1 >> A_2 \quad \text{or} \quad A_1 > 9A_2 \ . \tag{51}$$

The factor 9 is selected as an arbitrary limit. Using conditions (51) and (50) in (42), it follows that

$$\chi = (A_1/2A_3)^{1/2} \ . \tag{52}$$

(iii) Tafel line

Substituting value of χ from Eq. (52) and A_1 from Eq. (43) into Eq. (47) it follows that

$$i_c = FA_1 \tag{53}$$

or
$$i_c = FK_1 a_{H^+} \exp(-\Delta VpF/2RT) \ . \tag{54}$$

Differentiating ΔVp of Eq. (54) with respect to ln i_c, it follows that

$$-d\Delta Vp/d \ln i_c = 2RT/F \ . \tag{55}$$

Also it can be shown that

$$b = -dVp/d \ln i_c = -d\eta/d \ln i_c = RT/\beta\lambda F \ . \tag{56}$$

Therefore, when simple discharge is a rate determining step

$$b = 2RT/F$$

$$\alpha = \lambda\beta = 1/2 \; .$$

Since $$\lambda = 1, \; \beta = 1/2 \; . \qquad (57)$$

(I-2) Atomic Desorption is Rate Determining (Path B)

(i) General condition

Comparing with (50), the condition is

$$10A_3 < (A_1 + A_2) \; . \qquad (58)$$

(ii) Coverage of surface

Following the same idea used in obtaining Eq. (51)

$$9A_2 < A_1 \; . \qquad (59)$$

From Eq. (42) the value of χ is

$$\chi = \frac{-(A_1 + A_2) + \sqrt{(A_1 + A_2)^2 + 8A_1A_3}}{4A_3} \qquad (42)$$

$$= \frac{[-1 + (1 + (8A_1A_3)/(A_1 + A_2)^2)^{1/2}]}{(4A_3)/(A_1 + A_2)} \; . \qquad (60)$$

From condition (51), $(8A_1A_3)/(A_1 + A_2) < 1$, hence

$$\chi = -(A_1 + A_2)/(4A_3) + (A_1 + A_2)(1 + (4A_1A_3)/$$
$$(A_1 + A_2)^2)/4A_3 \qquad (61)$$

or $$\chi = A_1/(A_1 + A_2) \; . \qquad (62)$$

(iii) Tafel line

From Eqs. (43), (44), (47) and (62)

$$i_c = 2F10^{-18}k_3(A_1/(A_1 + A_2))^2 \qquad (63)$$

$$= 2Fk_3 10^{-18}[1/(1 + ((k_2 10^{-9})/k_1 a_{H^+})\exp(\Delta VpF/RT)]^2 \quad (64)$$

$$= 2Fk_3 10^{-18}[1 + ((k_2 10^{-9})/k_1 a_{H^+})\exp(\Delta VpF/RT)]^{-2} . \quad (65)$$

Therefore, $\ln i_c = \ln(2Fk_3 10^{-18}) - 2 \ln[1 + ((k_2 10^{-9})/k_1 a_{H^+})\exp(\Delta VpF/RT)$. (66)

Evaluation of $d(\Delta Vp)/d \ln i_c$ yields

$$-d(\Delta Vp)/d \ln i_c = \frac{1 + [(k_2 10^{-9})/(k_1 a_{H^+})]\exp(\Delta VpF/RT)}{[(2Fk_2 10^{-9})/(k_1 RT a_{H^+})]\exp(\Delta VpF/RT)} . \quad (67)$$

From Eq. (58), it is seen that the values of α and β are complex functions of potential and can be calculated from (58) by the use of (23) and (24), taking λ as 2 (since two electrons are involved for Path B).

Two important limiting conditions arise from Eq. (67).

Limiting condition 1

If $[(k_2 10^{-9})/(k_1 a_{H^+})]\exp(\Delta VpF/RT) > 10$. (68)

Then from Eq. (67)

$$-d(\Delta Vp)/d \ln i_c = RT/2F = b \quad (69)$$

where b is the Tafel slope. Therefore, comparing with the general form of Tafel slope, $b = RT/\lambda\beta F$, α is 2 and β is 1 because $\lambda = 2$. (70)

Limiting condition 2

If ΔVp tends to $-\infty$, $b \to \infty$ (71)

$\alpha \to o$ and $\beta \to o$. (72)

Inclusion of the limiting condition (68) in (65) gives

$$i_c = 2Fk_3[(k_1 a_{H^+})/k_2]^2 \exp(-2\Delta VpF/RT) \quad (73)$$

and of (71) in the same equation, gives

$$i_c = 2Fk_3 10^{-18} . \quad (74)$$

II Reaction Paths C and D

The source of protons is H_3O^+ and the electrochemical reaction is desorptive.

General kinetic equations

The reactions and velocities to be considered are

$$H_3O^+ + e + M \xrightarrow{v_1} MH_{ads} + H_2O \tag{75}$$

$$MH_{ads} + H_2O \xrightarrow{v_2} H_3O^+ + e + M \tag{76}$$

and

$$H_3O^+ + MH_{ads} + e \xrightarrow{v_4} H_2 + M + H_2O \ . \tag{77}$$

v_1 and v_2 are given by (38) and (39). v_4 is given by

$$v_4 = k_4 10^{-9} a_{H^+} \chi \exp(-\Delta VpF/2RT). \tag{78}$$

At the steady state

$$v_1 - v_2 - v_4 = 0 \tag{79}$$

From Eqs. (38), (39) and (78) value of χ is

$$\chi = A_1/(A_1 + A_2 + A_4) \tag{80}$$

where

$$A_4 = k_4 10^{-9} a_{H^+} \exp(-\Delta VpF/2RT) \ . \tag{81}$$

The current is $i_c = \lambda F v_4$

$$= \lambda F k_4 10^{-9} a_{H^+} \chi \exp(-\Delta VpF/2RT) \tag{82}$$

$$= 2F k_4 10^{-9} a_{H^+} \chi \exp(-\Delta VpF/2RT) \ . \tag{83}$$

From Eqs. (43), (44), (80) and (83)

$$i_c = \frac{2Fk_4 10^{-9} a_{H^+} \exp(-\Delta VpF/2RT) k_1 a_{H^+} \exp(-\Delta VpF/2RT)}{(k_1 a_{H^+} + k_4 10^{-9} a_{H^+}) \exp(-\Delta VpF/2RT) + 10^{-9} k_2 \exp(\Delta VpF/2RT)}$$

$$= \frac{2Fk_1k_4(a_{H^+})^2 10^{-9} \exp(-\Delta VpF/2RT)}{(k_1 a_{H^+} + k_4 10^{-9} a_{H^+}) + 10^{-9} k_2 \exp(\Delta VpF/RT)} \tag{84}$$

and from Eq. (84)

$$\frac{d(\Delta Vp)}{d \ln i_c} = \frac{1 + [(k_2 10^{-9})/(k_1 + k_4 10^{-9}) a_{H^+}] \exp(\Delta VpF/RT)}{-F/2RT[1 + [(k_2 10^{-9})/(k_1 + k_4 10^{-9}) a_{H^+}] \exp(\Delta VpF/RT)]}$$

$$-[(Fk_2 10^{-9}/(k_1 + k_4 10^{-9}) a_{H^+} RT) \exp(\Delta VpF/RT)] \ . \tag{85}$$

(II-1) Simple Discharge is Rate Determining (Path C)

(i) General condition

$$10(A_1 + A_2) < A_4 \tag{86}$$

(ii) Coverage of surface

From Eqs. (80) and (86)

$$\chi = A_1/A_4 \ . \tag{87}$$

From Eqs. (43) and (81)

$$\chi = (k_1)/(10^{-9} k_4) \ . \tag{88}$$

(iii) Tafel line

Condition (86) when put in Eq. (84) gives

$$i_c = 2Fk_1 a_{H^+} \exp(-\Delta VpF/2RT) \ . \tag{89}$$

This relation is very similar to that found for a rate determining discharge reaction followed by an atomic hydrogen desorption step. In Eq. (89)

$$\alpha = 0.5 \tag{90}$$

and since $\nu = 2$

$$\beta = 1/4 \ . \tag{91}$$

(II-2) Kinetics When Electrochemical Step is Rate Determining (Path D)

(i) General condition

$$10A_4 < A_1 + A_2 \tag{92}$$

(ii) Coverage of surface

Special case (a) $\quad 10A_1 < A_2$ (93)

From Eqs. (80), (92) and (93)

$$\chi = A_1/A_2 \tag{94}$$

Special case (b) $\quad 10A_2 < A_1$ (95)

From Eqs. (80), (92) and (95)

$$\chi \simeq 1 \tag{96}$$

(iii) Tafel line

Special case (a). Conditions (92) and (93) and Eq. (84) give

$$i_c = 2F(k_1/k_2)k_4(a_H+)^2\exp(-3\Delta VpF/2RT) \tag{97}$$

therefore, $\alpha = 3/2$

and $\quad \lambda = 2;\ \beta = 3/4\ .$ (98)

Special case (b). From conditions (92) and (95) and Eq. (84), it follows

$$i_c = 2Fk_4a_H+10^{-9}\ \exp(-\Delta VpF/2RT). \tag{99}$$

Therefore $\quad \alpha = 0.5;\ \beta = 1/4$ as $\lambda = 2$. (100)

Results of the derivations presented above for various reaction mechanisms are given in Table 1.

Table I. Characteristics of various mechanisms of cathodic hydrogen evolution in acid solutions

Mechanism	Conditions for Application	λ	With Symmetrical Energy Barrier α	β	$b = \frac{RT}{\lambda\beta F}$
Slow Discharge Fast Atomic Desorption (A)	$10(A_1 + A_2) < A_3$ $9A_2 < A_1$	1	1/2	1/2	2RT/F
Slow Atomic Desorption Fast Discharge (B)	$10A_3 < A_1 + A_2$ $9A_2 < A_1$	2	2	1	RT/2F
Slow Discharge Fast Electrochemical (C)	$10(A_1 + A_2) < A_4$	2	1/2	1/4	2RT/F
Slow Electrochemical Fast Discharge (D)	$A_1 + A_2 > 10A_4$				
	$A_2 > 10A_1$	2	3/2	3/4	2RT/3F
	$A_1 > 10A_2$	2	1/2	1/4	2RT/F

2.3 Stoichiometric Number, μ

The stoichiometric number is defined as the number of acts of the rate determining step accompanying one act of the overall hydrogen evolution reaction. .

The hydrogen evolution reaction may be represented in acid solutions by the overall reaction

$$2H_3O^+ + 2e \rightleftarrows H_2 \ .$$

If there is one step in the overall reaction which is rate determining, then the rate v_1 of the forward direction of this step, derived from Eq. (37), is

$$v_1 = a_1(kT/h)\exp[-(\Delta G_1^* + 2\beta(\Delta V_c - \zeta)(F/\mu))/RT] \tag{101}$$

where a_1 = product of the activities of reactants of the rate determining step at the site of reaction.

The analogous equation for the reverse reaction is

$$v_2 = a_2(kT/h)\exp[-(\Delta G_2^* - 2(1 - \beta)(\Delta V_c - \zeta)(F/\mu))/RT] \ . \tag{102}$$

The currents i_1 and i_2 corresponding to v_1 and v_2 are

$$i_1 = 2\varepsilon v_1/\mu$$

$$i_2 = 2\varepsilon v_2/\mu \tag{103}$$

where ε is the electronic charge. When $\Delta V_c = \Delta V_R$, $i_1 = i_2 = i_o$. In the general case, since $\Delta V_R + \eta = \Delta V_c$ and $i_c = i_1 - i_2$, it follows from Eqs. (101), (102), and (103) that

$$i_c = i_o[\exp(-2\beta\eta F/\mu RT) - \exp(2(1 - \beta)\eta F/\mu RT)] \ . \tag{104}$$

At values of η greater than zero, Eq. (104) reduces to

$$i_c = i_o \exp(-2\beta\eta F/\mu RT) \tag{105}$$

and when $\eta \to o$, Eq. (104) approximates to

$$i_c = -2i_o \eta F/\mu RT \ . \tag{106}$$

Differentiating and rearranging Eq. (106),

$$\mu = (-2i_o F/RT)(d\eta/di_c)_{\eta \to o} \ . \tag{107}$$

2.4 Deuterium Substitution

Several theories on the electrolytic hydrogen deuterium separation from aqueous acid or alkaline solutions have attributed the difference in rates of the electrolytic production of H_2, HD or D_2 primarily to the different zero-point energies of the OH or OD bonds undergoing dissociation in the proton or deutron transfer in the first simple discharge step, i.e.,

$$H_3O^+ + e + M \rightarrow MH_{ads} + H_2O$$

in the overall hydrogen evolution reaction at the electrode surface. This procedure is an over simplification and leads to values of the separation factor, S, which are not in good agreement with experiment for various metals and fails to explain the clear division of values of S determined for various metals in acid solutions into two groups.

In order to explain some of the differences between the theory and experiment, one or more of the following factors are to be considered.

1. Differences of hydration energy of the isotopic ions.
2. Relative concentrations of the discharged ions.
3. Difference of ionization potential of D and H.
4. Differences of entropy of activation for deuterium and hydrogen evolution.
5. The rate determining mechanism involved in the overall reaction.
6. Whether H_2 and HD are produced in the rate determining step or not.

By considering all the quantities which determine the heat contents of the initial, activated, and final states of various possible rate determining steps in the overall electrolytic H_2, HD and D_2 evolution reactions, it is shown that some important experimental facts can be explained.

2.4.1 Difference in Zero Point Energy

The major factor which contributes to the free energy difference is the difference in zero point energy between a bond to deuterium and the corresponding bond to hydrogen. The potential energy curves (Morse curves) for a bond to deuterium and a corresponding bond to hydrogen are essentially identical.

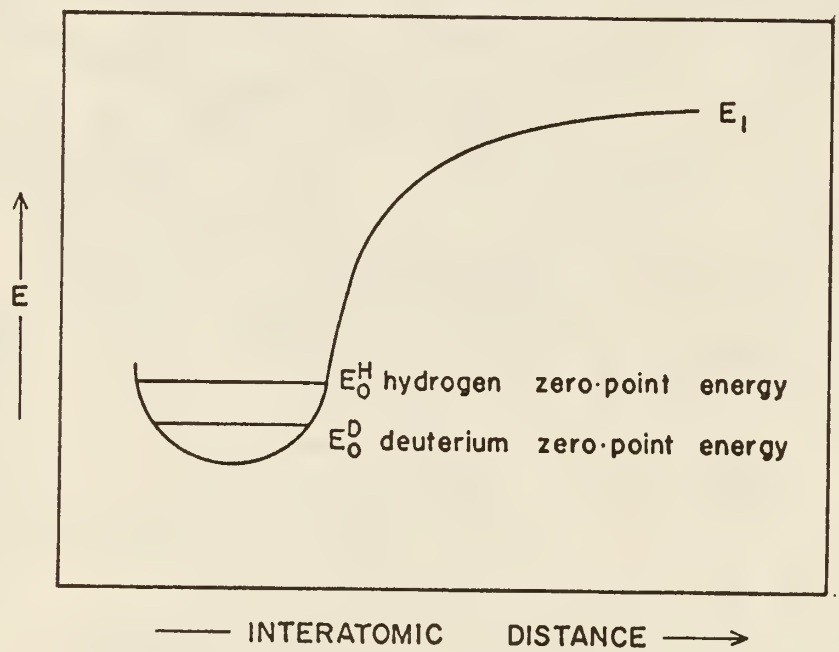

Fig. 2. Morse Curve Relating to Potential Energy to Interatomic Distance

The lowest energy level for any bond corresponds to $(1/2)h\nu$, where h is Planck's constant. This lowest energy level is known as the zero point energy. This corresponds to the vibrational energy of the bonds at absolute zero. At room temperature, approximately 99% of the bonds are in this vibrational energy level. There is a difference in zero point energy for a bond to hydrogen and the corresponding bond to deuterium. This arises from the effect of the difference in mass on the stretching frequencies. The shape of the bottom of the energy curve governs the force constant for the stretching vibration, and this is related to the frequency by Hooke's law

$$\nu = (1/2\pi)(K_F/\mu_m)^{1/2} \tag{108}$$

where K_F is the force constant and μ_m is the reduced mass, which is approximately equal to 1 and 2 for most hydrogen- and deuterium-containing bonds respectively.

The difference in zero point energy has two consequences. The first of these is a difference in dissociation energy for the hydrogen- and deuterium-containing bonds. The dissociation energy is the difference in energy between E_1 and the zero point energy in Fig. 2. Since the deuterium compound has lower zero point energy than the corresponding hydrogen compound, the deuterium compound will have a larger dissociation energy, and thus be more stable than its hydrogen analog. The remaining consequence can be explained by noting Fig. 3 in which the potential energy of the system is plotted against the distance along the reaction coordinate. Following the idea of activated complexes discussed in Section 2.1, if one assumes the bond undergoing reaction to be relatively weak in the activated complex in comparison to the bond in the reactants, the effect of zero point energy on the rate of reaction becomes apparent. The weak bond in the activated complex reflects a low force constant,

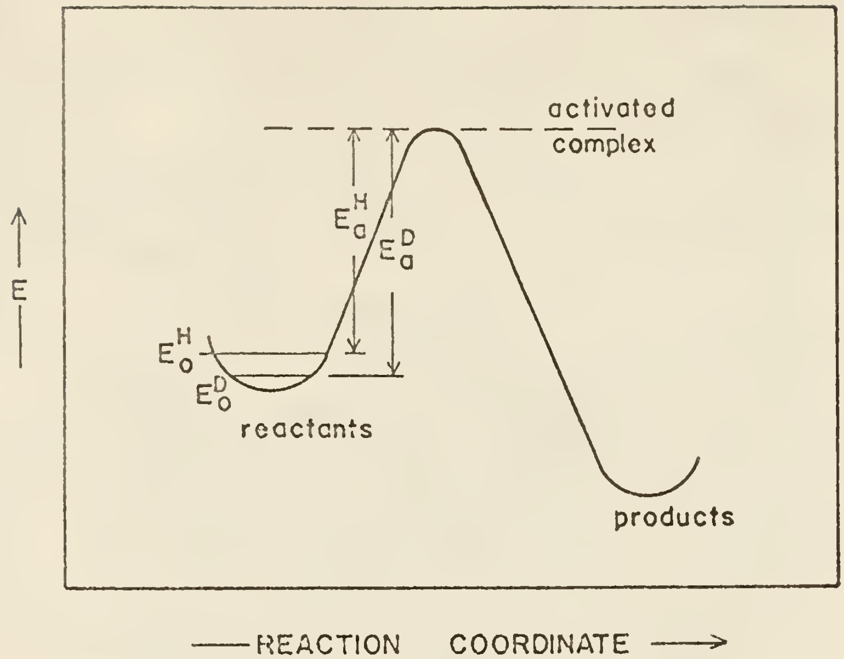

Fig. 3. Potential Energy Profile

and since the difference in zero point energy decreases with decreasing force constant, the difference in zero point energy for the bond in the activated complex will be small. Thus, the difference in zero point energy in the reactants will result in a larger energy of activation for the deuterium containing compound. In this reasoning it is assumed that the bonds in the molecule which do not participate in the reaction are not affected during the process. This appears to be a good approximation in most cases.

From the consideration of free energy, it would then appear that hydrogen-containing bonds would undergo reaction with more ease and at more rapid rates than corresponding deuterium bonds.

2.4.2 Separation Factor

The separation factor, S, is defined by

$$S = \frac{(C_H/C_D)_{II}}{(C_H/C_D)_I} \tag{109}$$

where C_H = concentration of hydrogen

C_D = concentration of deuterium

II = after the separation

and I = before the separation.

In electrolytic separation, II refers to the gas phase and I refers to the solution phase.

The ratio of H to D in the gas is related to the ratio of the currents for hydrogen and deuterium ion neutralization at a given metal-solution potential difference.

During the electrode process of separation of H and D, there is a definite change in free energy which can be written (14) as

$$\Delta F = \Delta F^\circ + RT \ln K \tag{110}$$

where ΔF = change in free energy of the reaction

ΔF° = change in free energy of the standard state of unit activity

R = gas constant

T = absolute temperature

and K = reaction constant.

For the case of equilibrium $\Delta F = 0$; therefore, $-\Delta F^\circ = RT \ln K$ or

$$K = \exp(-\Delta F^\circ/RT) \ . \tag{111}$$

Therefore, $$K = \frac{\pi_a(\text{Products})}{\pi_a(\text{Reactants})} = \exp(-\Delta F^\circ/RT) \ . \tag{112}$$

For the hydrogen reaction, since $\pi_a(\text{Products}) = (C_H)_{II}$

then, $$(C_H)_{II} = \pi_a(\text{H reactants})\exp(-\Delta F_H^\circ/RT) \; . \tag{113}$$

For the deuterium reaction

$$(C_D)_{II} = \pi_a(\text{D reactants})\exp(-\Delta F_D^\circ/RT) \; . \tag{114}$$

In the case of electrolytic separation, the change in the free energy of standard state, i.e., ΔF°, is due to the change in the free energy of activation for the rate determining H or D producing reactions and is denoted by $(\Delta G^\circ)^*$. Dividing (113) by (114) and writing

$$\Delta F^\circ = (\Delta G^\circ)^* \tag{115}$$

it follows that

$$(C_H/C_D)_{II} = \frac{\pi_a(\text{H reactants})}{\pi_a(\text{D reactants})} \exp[((\Delta G_D^\circ)^* - (\Delta G_H^\circ)^*)/RT] \; . \tag{116}$$

<u>Derivation of the separation factor using partition functions.</u>

The separation factor, S, which is due to the different energies of molecules can also be evolved from the point of view of partition functions. The partition function, Q, is defined by the relation

$$Q = g_o e^{-\varepsilon_o/kT} + g_1 e^{-\varepsilon_1/kT} + g_2 e^{-\varepsilon_2/kT} + \ldots \tag{117}$$

where ε_o, ε_1, and ε_2 are the energies of a single molecule in the various possible levels (15, 16) and g_o, g_1, are constants, or

$$Q = \sum_i g_i e^{-\varepsilon_i/KT} \; . \tag{118}$$

The entropy, s, is expressed in terms of the partition function (16) as

$$s = E/T + R \ln(Q/N) + R \tag{119}$$

where E = total energy

and N = Avogadro's number.

Using the thermodynamic definition

$$F' = E + PV - Ts \tag{120}$$

$$= E + RT - Ts \tag{121}$$

and combining Eqs. (119) and (121), it follows that

$$F' = -RT\ \ln(Q/N)\ . \tag{122}$$

The partition function Q is related to the partition functions based on the energy zero by the relation (16)

$$Q_{E_o} = Qe^{-E_o/RT} \tag{123}$$

Hence Eq. (122) can be written in terms of Q_{E_o} where E_o is the total energy based on energy zero

$$F = -RT\ \ln(Q/N) + E_o\ . \tag{124}$$

Using the superscript "o" when the substances are in their standard states

$$F^\circ = -RT\ \ln(Q^\circ/N) + E_o^\circ\ . \tag{125}$$

In a reaction $aA + bB \rightleftarrows lL + mM$

$$\Delta F^\circ = F^\circ_{Products} - F^\circ_{Reactants}$$

$$= -RT[\ln(Q^\circ/N)^l + \ln(Q^\circ/N)^m - \ln(Q^\circ/N)^a - \ln(Q^\circ/N)^b] \tag{126}$$

$$+ \ E^\circ_{o\ Products} - E^\circ_{o\ Reactants}$$

or $$\Delta F^\circ = -RT \quad \ln \frac{(Q^\circ/N)^l_L (Q^\circ/N)^m_M}{(Q^\circ/N)^a_A (Q^\circ/N)^b_B} + \Delta E^\circ_o \tag{127}$$

where $\Delta E^\circ_o = E^\circ_{o\ products} - E^\circ_{o\ reactants}$. Also

$$-\Delta F^\circ = RT\ \ln K\ . \tag{128}$$

Equating (127) and (128)

$$RT\ \ln K = RT\ \ln \frac{(Q^\circ/N)^l_L (Q^\circ/N)^m_M}{(Q^\circ/N)^a_A (Q^\circ/N)^b_B} - \Delta E^\circ_o \qquad (129$$

or $$K = \frac{(Q^\circ/N)^l_L (Q^\circ/N)^m_M}{(Q^\circ/N)^a_A (Q^\circ/N)^b_B} e^{-\Delta E^\circ_o/RT} . \tag{130}$$

In the case of formation of activated complex, X^*, by the reactants

$$A + B \rightleftarrows X^*$$

$$K = \frac{(Q^\circ/N)_{X^*}}{(Q^\circ/N)_A (Q^\circ/N)_B} \exp(-\Delta E^\circ_o/RT) \tag{131}$$

where ΔE°_o = heat of activation at absolute zero = ΔH^*_o because $\Delta PV = 0$ and

because $K = \pi_a(\text{Products})/\pi_a(\text{Reactants})$. (132)

The above equations are now used for H and D reactions. From Eq. (130)

$$\pi_a(\text{Products}) = (C_H)_{II}$$

$$= \pi_a(\text{H reactants}) \frac{(Q^\circ/N)_{X^*}}{\pi[(Q^\circ/N)_{\text{H reactants}}]} \exp(-\Delta H^*_{o,H}/RT) . \tag{133}$$

Similarly,

$$(C_D)_{II} = \pi_a(\text{D reactants}) \frac{(Q^\circ/N)_{X^*}}{\pi[(Q^\circ/N)_{\text{D reactants}}]} \exp(-\Delta H^*_{o,D}/RT) . \tag{134}$$

Therefore,

$$(C_H/C_D)_{II} = \frac{\pi_a(\text{H reactants})}{\pi_a(\text{D reactants})} \frac{[F^\circ_H/\pi_f(\text{H reactants})]}{[F^\circ_D/\pi_f(\text{D reactants})]} \exp[(\Delta H^*_{o,D} - \Delta H^*_{o,H})/RT]$$

or $$S = (C_D/C_H)_I \frac{\pi_a(\text{H reactants})}{\pi_a(\text{D reactants})} \frac{[F^\circ_H/\pi_f(\text{H reactants})]}{[F^\circ_D/\pi_f(\text{D reactants})]} \exp[(\Delta H^*_{o,D} - \Delta H^*_{o,H})/RT] \tag{135}$$

where π_f = the product of partition functions of H and D containing reactants

F°_H = total partition function for the activated state involving H

F°_D = total partition function for the activated state involving D

2.4.3 Proton and Deuteron Affinities of H_2O and D_2O

The proton affinity, i.e., the enthalpy change in the reaction

$$H^+_{gas} + H_2O_{gas} \rightarrow H_3O^+_{gas}$$

is -182 Kcal/mole (17).

The deuteron affinity of H_2O and D_2O differs from the proton affinity of water on account of the different zero point vibrational energies of the bonds in D_2O and H_2O and D_3O^+, H_2DO^+, and H_3O^+.

The difference of proton and deuteron affinities of H_2O is represented by $\Delta H_{(D^+ - H^+)}$ (18) and is given by

$$\Delta H_{(D^+ - H^+)} = [(\sum_1^6 (1/2)h\nu_o)_{DH_2O^+} - (\sum_1^3 (1/2)h\nu_o)_{H_2O}] - [(\sum_1^6 (1/2)h\nu_o)_{H_3O^+} - (\sum_1^3 (1/2)h\nu_o)_{H_2O}] \quad (136)$$

The terms are evaluated from the spectroscopic ground state frequencies for the 6 vibrational modes of the oxonium ion and three of H_2O molecule. The number of modes of vibration are given by (3n - 6), where n is the number of atoms in the ion or molecule.

After substituting the values for the zero point energies reported by Dennison (19) Eq. (136) gives

$$\Delta H_{(D^+ - H^+)} = (19.60 - 12.70) - (21.40 - 12.70) \quad (137)$$

$$= -1.8 \text{ Kcal/mole.}$$

In the presencé of excess of H_2O at the start of a normal separation experiment, both the ions H_3O^+ and DH_2O^+ will be almost exclusively solvated by H_2O molecules, and the difference of overall solvation energy of D^+ and H^+ in excess H_2O will be equal to the difference of deuteron and proton affinity of H_2O. Since H_3O^+ and DH_2O^+ have the same diameter (the mean intermolecular distances between O and H, and O and D atoms in the OH and OD bonds differ by less than 0.001 A° in the ground state) and charge; hence the solvation energies of H_3O^+ and DH_2O^+ will be almost identical.

2.4.4 Solvation Energy of Ions

Solvation energy of ions in a medium of dielectric constant d may be regarded as equivalent to the difference in the electrostatic energy of a gaseous ion and that of an ion in the medium. In order to evaluate this quantity theoretically, use is made of the method by Born (20); the free energy increase accompanying the charging of a single gaseous ion in medium of dielectric constant unity, is $z^2e^2/2r$, (13), where ze is the charge carried by the ion and r is its effective radius, the ion being treated as a conducting sphere. If the same ion is charged in a medium of dielectric constant d, the free energy change is $z^2e^2/2dr$, and so the increase of free energy, ΔG, accompanying the transfer of 1 gm mole of the gaseous ion to that medium, which is the free energy of solvation, is given by the Born equation

$$\Delta G = [(-Nz^2e^2)/(2r)](1 - 1/d) \quad . \tag{138}$$

The difference of overall solvation energy of H^+ in H_2O and D^+ in D_2O can also be obtained (21) from the electromotive force of the cell,

$$\text{Pt } (H_2) \;\Big|\; \text{HCl (1N) in } H_2O \;\Big|\; \text{DCl (1N) in } D_2O \;\Big|\; D_2 \text{ (Pt)}$$

which is -0.002 V (21).

To estimate the liquid junction potential in the above cell, use is made of the Henderson equation (13),

$$E_L = (RT/F)\frac{(U_1 - V_1) - (U_2 - V_2)}{(U'_1 + V'_1) - (U'_2 + V'_2)} \ln[(U'_1 + V'_1)/(U'_2 + V'_2)] \tag{139}$$

$$U_1 = \Sigma(C_+U_+)_1 \quad ; \quad V_1 = \Sigma(C_-U_-)_1$$

$$U_1' = \Sigma(C_+Z_+U_+)_1 \qquad V_1' = \Sigma(C_-Z_-U_-)_1 \tag{140}$$

where C_+ and C_- refer to the concentrations of the cations and anions respectively, in gram ions per litre, U_+ and U_- are the corresponding mobilities and Z_+ and Z_- their valencies and where the suffixes 1 and 2 refer to the ions in solutions 1 and 2 respectively.

In the present case, solution 1 is a $HCl\text{-}H_2O$ solution and solution 2 is a $DCl\text{-}D_2O$ solution, $Z_+ = Z_- = 1$, hence

$$U_1 = U_1' \quad ; \quad V_1 = V_1'$$

$$U_2 = U_2' \quad ; \quad V_2 = V_2' \quad . \tag{141}$$

Eq. (139) reduces to

$$E_L = (RT/F)\frac{(U_1 - V_1) - (U_2 - V_2)}{(U_1 + V_1) - (U_2 + V_2)}\ln[(U_1 + V_1)/(U_2 + V_2)] \tag{142}$$

$$U_1 = C_{H^+}U_{H^+} \quad ; \quad U_2 = C_{D^+}U_{D^+}$$

$$V_1 = C_{Cl^-}U_{Cl^-} \quad ; \quad V_2 = C_{Cl^-}U_{Cl^-} \quad . \tag{143}$$

Since the $HCl\text{-}H_2O$ and $DCl\text{-}D_2O$ solutions are of the same concentrations, it is assumed that

$$C_{H^+} = C_{Cl^-}$$

$$C_{D^+} = C_{Cl^-}$$

$$C_{H^+} = C_{D^+} \quad . \tag{144}$$

Eq. (142) then reduces to

$$\begin{aligned} E_L &= (RT/F)\ln[(U_1 + V_1)/(U_2 + V_2)] \\ &= (RT/F)\ln[(C_{H^+}U_{H^+} + C_{Cl^-}U_{Cl^-})/(C_{D^+}U_{D^+} + C_{Cl^-}U_{Cl^-})] \\ &= (RT/F)\ln[U_{H^+} + U_{Cl^-})/(U_{D^+} + U_{Cl^-})] \quad . \end{aligned} \tag{145}$$

Defining transference numbers for hydrogen and deuterium ions as

$$(t_+)_H = U_{H^+}/(U_{H^+} + U_{Cl^-})$$

$$(t_+)_D = U_{D^+}/(U_{D^+} + U_{Cl^-}) \quad (146)$$

and substituting Eq. (146) into Eq. (145) it follows that

$$E_L = (RT/F)\ln[(U_{H^+}/(t_+)_H)/(U_{D^+}/(t_+)_D)] \ . \quad (147)$$

Using the mobility data given in references (22) and (23) and the transference number data given in reference (24)

$$E_L = .007 \text{ V}. \quad (148)$$

The corrected E.M.F., therefore, is -.009 V and corresponds to a standard free energy change, ΔG_o, given by

$$-\Delta G_o = nFE = \frac{-0.009 \times 96500}{1000 \times 4.183} = -0.21 \text{ Kcal/mole} \ . \quad (149)$$

This can be equated approximately to the heat content change in the cell reaction, $\Delta G°$ cell.

The difference of overall heat of solvation $\Delta[\Delta H_{s,D_3O^+} - {}_{H_3O^+}]$ of D^+ in D_2O and H^+ in H_2O is then given by

$$-\Delta(\Delta H_{s,D_3O^+} - {}_{H_3O^+}) = \Delta[(1/2)D^\circ_{D_2} - {}_{H_2}] + \Delta[I_{D} - {}_{H}] + \Delta G° \text{ cell} \quad (150)$$

where $\Delta[(1/2)D^\circ_{D_2} - {}_{H_2}]$ is the difference between the bond dissociation energies of D_2 and H_2, $\Delta[I_D - {}_H]$ is the difference between the ionization potentials of D and H atoms.

Using the values shown in Table II and the value of $\Delta G°$cell calculated above gives

$$\Delta[\Delta H_{s,D_3O^+} - {}_{H_3O^+}] = -1.2 \text{ Kcal/mole} \ . \quad (151)$$

2.4.5 Rate Determining Steps

As indicated in Section 2.2, the following reactions have been suggested as rate determining steps in hydrogen evolution at various metals on the basis of modern experimental data obtained in ultra-purified solutions.

I $H_3O^+ + M + e^- \rightarrow H_2O + MH_{ads}$: Simple discharge or slow discharge

II $H_3O^+ + MH_{ads} + e^- \rightarrow M + H_2 + H_2O$: Electrochemical desorption or atom ion desorption

III $MH_{ads} + MH_{ads} \rightarrow H_2$: Atom desorption or atom recombination

Similarly analogous reactions are suggested for partially and completely deuterated species.

Case I: Simple Discharge

(a) Simple discharge in water containing the normal isotopic mixture of H and D.

The isotopic molecules are H_2O, HDO and D_2O and oxonium ions are H_3O^+, D_3O^+, H_2DO^+ and HD_2O^+.

The D content of normal water is 0.015 mole % and the equilibrium constant for the reaction

$$H_2O + D_2O \rightarrow 2HOD$$

is 3.8 at 25°C (25) which gives the equilibrium activities of the isotopic water species as follows

$$a_{H_2O} = 55 \text{ mole/liter}$$

$$a_{HOD} = 1 \times 10^{-2}$$

$$a_{D_2O} = 5 \times 10^{-7} \quad . \tag{152}$$

For calculation of S, the separation factor, from Eq. (135) the ratios of pairs of equilibrium activities of isotopic oxonium ions are required. These ratios can be calculated from the following equations if the ratios of the respective equilibrium constants can be obtained.

$$a_{H_3O^+} = K_1 a_{H^+} a_{H_2O}$$

$$a_{DH_2O^+} = K_2 a_{D^+} a_{HOD}$$

$$a_{D_2HO^+} = K_3 a_{D^+} a_{HOD}$$

$$a_{D_3O^+} = K_4 a_{D^+} a_{D_2O} \quad . \qquad (153)$$

The ratios for K_1 and K_2 are given by

$$K_1/K_2 = \exp[(-(\Delta G^\circ_{s,H_3O^+} - \Delta G^\circ_{s,DH_2O^+}))/RT] \qquad (154)$$

where ΔG_s is the standard free energy of solvation in water of the proton or deuteron in the form of the various oxonium ions (18).

For the isotopic species, differences of free energy of solvation are primarily due to the differences of zero point energies of the ions, so that differences of free energy of solvation of H^+ and D^+ can be identified approximately with differences in corresponding heats of solvation calculated above. For example, in 0.1N acid solution, containing H_2O, HDO and D_2O, the activities of the oxonium ions are

$$a_{H_3O^+} = 10^{-1} \text{ (mole/liter)}$$

$$a_{DH_2O^+} = 3.8 \times 10^{-4} \text{ (mole/liter)} \qquad (155)$$

and $a_{D_2HO^+}$ is of the order of magnitude 10^{-8} and $a_{D_3O^+}$ is of the order of magnitude 10^{-12} (mole/liter) so that only H_3O^+ and DH_2O^+ need be considered as sources of protons or deuterons in acid solutions.

The two reactions whose rates must be compared, therefore, are

$$H_3O^+ + e^- + M \rightarrow MH_{ads} + H_2O \tag{156}$$

and

$$DH_2O^+ + e^- + M \rightarrow MD_{ads} + H_2O \quad . \tag{157}$$

Since thermodynamic quantities other than the zero point energies enter into the calculation of the different heats of activation for proton and deuteron discharge, it is therefore convenient to refer the total heat content of reactants and of products to that of the reference state, $1/2\ H_2 + H_2O + M$ in the case of reaction (156) and to that of $1/2\ D_2 + H_2O + M$ in the case of reaction (157) through the Born-Haber cycles.

Cycle I

$1/2\ H_2 + H_2O + M \rightarrow H + H_2O + M$	$1/2\ D^\circ_{H_2}$
$H + H_2O + M \rightarrow H^+ + e^- + H_2O + M$	I_H
$H^+ + e^- + H_2O + M \rightarrow H_3O^+ + e^-_M + M$	$\Delta H_{sH^+,H_2O} - \phi_M$

$$1/2\ H_2 + H_2O + M \rightarrow H_3O^+ + e^-_M + M$$

Reference state $\rightarrow$ Initial state of reaction (156)

$$(\Delta H_i)_H = 1/2\ D^\circ_{H_2} + I_H + \Delta H_{sH^+,H_2O} - \phi_M$$

Cycle II

$$1/2\ H_2 + H_2O + M \rightarrow H_2O + MH_{ads}$$

Reference state $\rightarrow$ Final state of reaction (156)

$$(\Delta H_f)_H = 1/2\ D^\circ_{H_2} + \Delta H_{adsH}$$

An alternative representation of the above two cycles is

Cycle I

$$
\begin{tikzcd}
 & & {[H^+ + e + H_2O + M]} \arrow[ddr, "\Delta H_{sH^+,H_2O} - \phi_M"] & \\
 & {[H + H_2O + M]} \arrow[ur, "I_H"] & & \\
{[1/2\ H_2 + H_2O + M]} \arrow[ur, "1/2\ D^\circ_{H_2}"] \arrow[rrr, "(\Delta H_i)_H"] & & & {[H_3O^+ + e_M + M]}
\end{tikzcd}
$$

Reference state | Initial state of (156)

and

Cycle II

$$
\begin{tikzcd}
 & {[H + H_2O + M]} \arrow[dr, "\Delta H_{adsH}"] & \\
{[1/2\ H_2 + H_2O + M]} \arrow[ur, "1/2\ D^\circ_{H_2}"] \arrow[rr, "(\Delta H_f)_H"] & & {[H_2O + MH_{ads}]}
\end{tikzcd}
$$

Reference state | Final state of (156)

For deuterium entities the Born-Haber cycles are

Cycle I

$$
\begin{tikzcd}
 & & {[D^+ + e^- + H_2O + M]} \arrow[ddrr, "\Delta H_{sD^+,H_2O} - \phi_M"] & & \\
 & {[D + H_2O + M]} \arrow[ur, "I_D"] & & & \\
{[1/2\ DH + H_2O + M]} \arrow[ur, "1/2\ D^\circ_{DH}"] \arrow[rrrr, "(\Delta H_i)_D"] & & & & {[DH_2O^+ + e_M + M]}
\end{tikzcd}
$$

Reference state

Initial state of reaction (157)

Cycle II

$$
\begin{tikzcd}
 & {[D + H_2O + M]} \arrow[dr, "\Delta H_{adsD}"] & \\
{[1/2\ DH + H_2O + M]} \arrow[ur, "1/2\ D^\circ_{DH}"] \arrow[rr, "(\Delta H_f)_D"] & & {[MD_{ads} + H_2O]}
\end{tikzcd}
$$

In these cycles, ΔH_i and ΔH_f are the heat content changes in the formation of the initial and final states from the reference state; $\Delta H_{sH^+,H_2O}$ is the heat of solvation of H^+ in H_2O, ΔH_{adsH} is the heat of adsorption of H at the metal surface and ϕ_M is the work function of the metal. The values of the terms are given in Table II.

As shown in Table II heat of solvation of H^+ in H_2O is -263 ± 13 Kcal/mole. The heat of solvation of D^+ can, therefore, be taken as $-263 - 1.8$ (see section above).

Using the data given in Table II

$$(\Delta H_i)_H = 101.6 - \phi_M \; ; \; (\Delta H_i)_D = 100.3 - \phi_M \; . \tag{158}$$

As seen (ΔH_i) values for H and D differ by 1.3 Kcal/mole, but this is also the difference between the zero point energies of the OH^+ and OD^+ bonds in H_3O^+ and H_2DO^+ ions in the initial state of the reaction. The minima of the potential energy curves for proton and deutron transfer from H_3O^+ or DH_2O^+ ions, respectively, therefore lie at the same potential energy. The minima for the final state curves differ in energy by the quantities ΔQ (see Appendix D). The difference in heats of activation for proton and deuteron transfer would, therefore, be equal to the difference in ΔH_i values for H and D, plus $\beta\Delta Q$, where $\beta = 0.5$ is the symmetry factor. An additional effect arises due to the slightly different shapes of the Morse curves for H^+ and D^+ dissociation from H_3O^+ and H_2DO^+, respectively. Evaluation, as described by Parsons and Bockris, (28), of the Morse constants "A" for these dissociation processes, gives

$$A_{H^+H_2O} = 1.62 \times 10^8 \quad \text{and} \quad A_{D^+H_2O} = 1.65 \times 10^8 \text{cm}^{-1} \; . \tag{159}$$

Substituting the above values of "A" into the Morse equation using the heats of solvation and zero point energies given in Table II for the $H^+ - H_2O$ and

Table II. Energy quantities used in the calculations

Quantity	Value in Kcal/mole	Reference
Ionization potential of H or D	$I_H = 313.00$; $I_D = 313.09$	(21)
Bond dissociation energy D° of		
H_2	$D_{H°} = 103.12$	(26)
HD	$D_{HD°} = 103.94$	(26)
D_2	$D_{D_2} = 104.92$	(26)
Proton affinity of water	-182	
Deuteron affinity of water	-183.8	(27,28)
Total heat of solvation of H^+ in H_2O	-263 ± 13	(29)
Total heat of solvation of D^+ in H_2O	-264.8	(27,28)
Total heat of solvation of D^+ in D_2O	-264.2	(27,28)
OH bond dissociation energy in H_2O	120	(30)
OD bond dissociation energy in HOD	121.5	(30)
Heat of ionization of H_2O in H_2O	13.50	(31)
Heat of ionization of HOD in H_2O (to give $H_2DO^+ + OH^-$)	13.89	(18)
Heat of ionization of D_2O in D_2O	14.50	(27)
Bond dissociation energy of		
CuH, CuD	$D^{\circ}_{CuH} = 66.8$; $D^{\circ}_{CuD} = 67.6$	(32)

Table II (continued)

Quantity	Value in Kcal/mole	Reference
AgH, AgD	$D^\circ_{AgH} = 57.7$; $D^\circ_{AgD} = 58.4$	(33)
PbH, PbD	$D^\circ_{PbH} = 37.0$; $D^\circ_{PbD} = 37.6$	(33)
HgH, HgD	$D^\circ_{HgH} = 57.0$; $D^\circ_{HgD} = 57.5$	(28)
NiH	$D^\circ_{NiH} = 71.0$	(33)
Zero point energy of		
CuH, CuD	$E^\circ_{CuH} = 2.78$; $E^\circ_{CuD} = 1.99$	
AgH, AgD	$E^\circ_{AgH} = 2.53$; $E^\circ_{AgD} = 1.79$	
PbH, PbD	$E^\circ_{PbH} = 2.20$; $E^\circ_{PbD} = 1.70$	
HgH, HgD	$E^\circ_{HgH} = 1.99$; $E^\circ_{HgD} = 1.43$	
NiH, NiD	$E^\circ_{NiH} = 2.27$; $E^\circ_{NiD} = 1.61$	(33)
Zero point energy of OH^+ bond in H_3O^+	5.0	(28)
Zero point energy of OD^+ bond in H_2DO^+	3.73	(28)

$D^+ - H_2O$ interaction, show that the Morse function for the dissociation of D^+ from H_2O rises more steeply than that for H^+. Potential energy diagrams show that in the activated state of the discharge reaction, the proton or deuteron bond to oxygen has to be stretched by about 0.2A° from the equilibrium separation. At this distance, the Morse curve for the dissociation of D^+ from DH_2O^+ is 0.6 Kcal higher than that for H^+ from H_3O^+ (18). With $\beta = 0.5$ the activation energy for D^+ transfer will hence be about 0.3 Kcal higher than that for H^+ on this account. The total difference of heat of activation is therefore

$$(\Delta H_D^* - \Delta H_H^*) = 1.3 + 1/2(0.36) + 1/2(0.60) = 1.78 \text{ Kcal/mole.} \qquad (160)$$

Using the ratio $C_D/C_H = 1/5500$ in ordinary water solutions; $a_{H_3O^+}/a_{DH_2O^+} = 10^{-1}/3.8 \times 10^{-4}$ as shown above in Eq. (155) and the fact that the probability of proton being discharged from H_3O^+ is 3 times that of a deuteron from DH_2O^+ in the double layer (34), the value of S is given by

$$S = (1/5500)(10^{-1}/3.8 \cdot 10^{-4})\ 3 \exp(1.78/RT)$$
$$= 2.9 \qquad . \qquad (161)$$

(b) Discharge in water containing either pure H_2O and protons or pure D_2O and deuterons.

Here the relative ratios of the simple discharge reaction, from H_3O^+ in H_2O and from D_3O^+ in D_2O for the same ionic concentrations, are compared.

$$H_3O^+ + e + M \rightarrow H_2O + MH_{ads} \qquad \text{I}$$

$$D_3O^+ + e + M \rightarrow D_2O + MD_{ads} \qquad \text{II}$$

1/2 $H_2 + H_2O + M$ is taken as the reference state for reaction I and 1/2 D_2 + $D_2O + M$ as the reference rate for reaction II. For reaction I $(\Delta H_i)_H$ = $101.56 - \phi_M$ as calculated above. For reaction II, Born-Haber cycles are

$$
\begin{tikzcd}
 & & D^+ + D_2O + M \arrow[ddr, "\Delta H_{sD^+,D_2O} - \phi_M"] & \\
 & D + D_2O + M \arrow[ur, "I_D"] & & \\
1/2\ D_2 + D_2O + M \arrow[ur, "1/2\ D^\circ_D"] \arrow[rrr, "(\Delta H_i)_D"] & & & D_3O^+ + M + e
\end{tikzcd}
$$

$$
\begin{aligned}
(\Delta H_i)_D &= 1/2(D^\circ_D) + I_D + \Delta H_{sD^+,D_2O} - \phi_M \\
&= 1/2(104.92) + 313.09 - 2.64.2 - \phi_M \\
&= 101.35 - \phi_M
\end{aligned}
$$

The difference (101.56 - 101.35) = <u>0.21</u> is not equal to the difference in zero point energy. Therefore the minima of the initial state potential energy curves differ by the difference of zero point of OH bond in H_3O^+ and OD bond in D_3O^+. The minima of the final state potential energy curves differ by 0.36 (Table III). Hence

$$
\begin{aligned}
(\Delta H^*_D - \Delta H^*_H) &= 0.21 + 1/2[(1.27 - .21) + (0.56 - 0.2)] + 1/2(0.60) \\
&= 1.22 \text{ Kcals/mole} \quad . \qquad (162)
\end{aligned}
$$

The activity ratio factor $a_{H_3O^+}/a_{D_3O^+}$ and the partition function ratios are both unity. Hence S from Eq. (135) is given by

$$
\begin{aligned}
S &= \exp((1.2 \times 1000)/(1.987 \times 298)) \\
&= 7.7 \qquad (163)
\end{aligned}
$$

Table III. Zero point energies and (ΔH_f) values for the simple discharge reaction at various metals

MH/MD	(ΔH_f)	Zero point energy E_o of MH or MD	$\Delta E_{0\ MH-MD}$	Difference ΔQ of depth of MH/MD p.e. curve minima
HgH	-5.4	1.99	0.56	0.36
HgD	-5.6	1.43	-	-
CuH	-15.2	2.78	0.79	0.39
CuD	-15.6	1.99	-	-
AgH	-6.1	2.53	0.74	0.44
AgD	-6.4	1.79	-	-
PbH	14.6	2.20	0.64	0.44
PbD	14.4	1.60	-	-

Case II: Electrochemical Desorption

(a) Discharge in water containing the normal isotopic mixture of H and D.

The following reactions are possible.

$$H_3O^+ + e + MH_{ads} \rightarrow H_2 + M + H_2O \qquad \mathrm{I}$$

$$DH_2O^+ + e + MH_{ads} \rightarrow HD + M + H_2O \qquad \mathrm{II}$$

$$H_3O^+ + e + MD_{ads} \rightarrow HD + M + H_2O \qquad \mathrm{III}$$

Here the heat contents of states in the reactions are referred to that of $H_2 + H_2O + M$ or $HD + H_2O + M$. The Born-Haber cycle for the initial state of reaction I is

$$\begin{tikzcd}
 & & H^+_{gas} + e + H_{gas} + M + H_2O \arrow[ddrr, "\Delta H_{sH^+,H_2O} + \Delta H_{adsH} - \phi_{MH}"] & & \\
 & 2H_{gas} + M + H_2O \arrow[ur, "I_H"] & & & \\
H_{2\ gas} + M + H_2O \arrow[ur, "D^\circ_{H_2}"] \arrow[rrrr, "(\Delta H_i)"] & & & & H_3O^+ + MH_{ads} + e_M
\end{tikzcd}$$

$$(\Delta H_i)_H = D^\circ_{H_2} + I_H + \Delta H_{sH^+,H_2O} + \Delta H_{adsH} - \phi_{MH}$$

Substituting the values for example for Ag

$$= 103.12 + 313 + (-263) + (-57.7) - \phi_{MH}$$

$$= 95.42 - \phi_{MH} \quad . \tag{164}$$

For a similar cycle for reaction II

$$(\Delta H_i)_D \text{ via } DH_2O^+ = D^\circ_{HD} + I_D + \Delta H_{sD^+,H_2O} + \Delta H_{adsH} - \phi_{MH}$$

$$= 94.53 - \phi_{MH} \quad . \tag{165}$$

and analogously for reaction III

$$(\Delta H_i)_D \text{ via } MD_{ads} = D^\circ_{HD} + I_H + \Delta H_{sH^+,H_2O} + \Delta H_{adsD} - \phi_{MH}$$

$$= 95.54 - \phi_{MH} \quad . \tag{166}$$

The heat contents of the final states are those of physically adsorbed H_2 at the metal for reaction I, or HD for II and III, and do not differ significantly. However, the minima of the final state potential energy curves for the formation of H_2 and HD will differ by the difference of the zero point energies of H_2 and HD, i.e., by 0.82 Kcal/mole which is the difference in dissociation energies of H_2 and HD. With $\beta = 0.5$, this gives a contribution of 0.41 Kcal/mole to the difference of heat of activation for H_2 and HD liberation by the electrochemical desorption mechanism. Similarly, for reactions I and II, the difference of the minima of the initial state curves will be equal to the difference of heat contents for the two initial states (namely, 95.42 - 94.53 Kcal/mole) minus the difference of zero point energies of the OH^+ and OD^+ bonds (namely, 1.27 Kcal/mole) i.e., 0.38 Kcal/mole, the curve for the D^+ transfer being the higher. Including the effect (0.6 βKcal) due to the difference of Morse functions for H^+ and D^+ dissociation, the total difference of heat of activation between reactions I and II will be

$$95.42 - 94.53 + 1/2(0.82) + 1/2(0.38) + 1/2(0.6) = 1.8 \text{ Kcal/mole} \quad .$$

With $a_{H_3O^+}/a_{H_2DO^+}$, the ratio, r, of rates of H_2 and HD production by reactions I and II respectively, is

$$r = 2.64 \times 10^2 \exp(1800/591) = 1.68 \times 10^4 = v_{H_2}/v_{HD} \qquad (167)$$

where v_{H_2} and v_{HD} are the velocities of production of H_2 and HD. The value of r is related to separation factor, S, by relation

$$S = (C_D/C_H)_{soln} \frac{v_{H_2} + (1/2)v_{HD}}{(1/2)v_{HD}} = (C_D/C_H)_{soln}(2r + 1) \ . \qquad (168)$$

Since in the production of HD, one H atom accompanies each D atom liberated. If $v_{H_2} >> v_{HD}$, as in the case considered above

$$S = (C_D/C_H)_{soln} \frac{2v_{H_2}}{v_{HD}} = (C_D/C_H)_{soln} \ 2r$$

$$= (1/5500) \times 2 \times 1.68 \times 10^4 = 6.1 \qquad (169)$$

i.e. almost twice the value arising if simple discharge were rate determining. In the calculation of S it has been assumed that the ratio of H_{ads} to D_{ads} is equal to the ratio of activities of H_3O^+ and H_2DO^+ in the solution. When the electrochemical desorption (III) is rate determining but faster than

$$MH_{ads} + MH_{ads} \rightarrow 2M + H_2 \ ,$$

the steady state concentration of adsorbed H has been calculated by Conway (18) and the value of S then calculated for this mechanism was 0.7, i.e., a value not observed experimentally. Hence atomic desorption is an unlikely path in HD evolution. However, the conditions for which S would be 0.7, are limiting and correspond to those for which Tafel slope of 0.038 for the electrochemical desorption mechanism is predicted (35), i.e., almost twice that arising if simple discharge were rate determining.

(b) Discharge of H_3O^+ and D_3O^+ ions in pure H_2O and D_2O respectively at the same acid concentration.

For this case, the reactions are

$$H_3O^+ + e + MH_{ads} \rightarrow H_2 + H_2O + M \qquad \text{I}$$

$$D_3O^+ + e + MD_{ads} \rightarrow D_2 + D_2O + M \ . \qquad \text{IV}$$

$(\Delta H_i)_H$ for reaction I, at silver, is 95.42 - ϕ_{AgH} Kcal/mole and for reaction IV, $(\Delta H_i)_D$ = 104.92 + 313.09 - 58.4 - 264.2 = 95.41 - ϕ_{AgD}. The zero point energy levels for the two initial states are therefore coincident, so that the minima of the initial state potential energy curves will differ by 1.27 Kcal/mole, that for D_3O^+ being higher. The minima of the final state potential energy curves will differ by the difference of zero point energy of H_2 and D_2, namely, 1.80 Kcal/mole. The heats of activation hence differ by

$$\Delta H_D^* - \Delta H_H^* = (95.42 - 95.41) + 1/2(1.27) + 1/2(1.80)$$

$$= 1.545 \text{ Kcal/mole} \ . \qquad (170)$$

The activity ratio $a_{H_3O^+}/a_{D_3O^+}$ is unity and the partition function ratio in Eq. (135) is 2 for the above case (18).

The hypothetical separation factor arising under the limiting conditions of acid solutions in pure H_2O and D_2O is, therefore

$$S = 2 \exp[1545/RT] = 27 \ . \qquad (171)$$

Case III: Atomic Desorption (or Atomic Recombination)

(a) Discharge in water containing the normal isotopic species of H and D. The reactions in ordinary water solutions in this case are

$$MH_{ads} + MH_{ads} \rightarrow 2M + H_2 \qquad \text{I}$$

$$MH_{ads} + MD_{ads} \rightarrow 2M + HD \ . \qquad \text{II}$$

At high surface coverage the difference of activation energy for reactions I and II is determined by the difference between the zero point energies of one MH_{ads} and one MD_{ads} bond. No data for the vibrational frequency of PtH (for which it is known that the above reaction is rate determining (18)) is available, but it is probably close to that for NiH, namely $\nu_{oNiH} = 4.75 \times 10^{13}$ and $\nu_{oNiD} = 3.36 \times 10^{13}$/sec.

The partition function ratio is 4/3 (18) so that the ratio of the rate of evolution of H_2 to that of HD is

$$r = (4/3)\exp[1/2((h\nu_o)_{NiH} - 1/2(h\nu_o)_{NiD})/kT] = 4.1 \qquad (172)$$

where h = Planck's constant = 6.625×10^{-27} ergs

k = Boltzmann constant = 1.38×10^{-16} ergs/deg

and since S = (2r + 1) as shown in Eq. (168), therefore S = 9.2. On an activated platinum surface in 1.5 N sulphuric acid, the experimental value of S is 6.4 (36, 37). Lower values have also been reported and it has been suggested that these arise not from an electrolytic separation, but because the $HDO + H_2 \rightleftarrows HD + H_2O$ equilibrium is set up at the catalytically active metal; this is disproved, however, by the work of Okamoto (38). The value calculated is an upper limit, since the heat of adsorption of H is diminished as the coverage of the metal by H approaches saturation, so that the zero point energies of the MH bonds would be expected to be lowered proportionally. Smaller values of S would hence arise; the minimum value, when the exponential in Eq. (172) is unity, is 2.7.

(b) When atomic desorption reaction takes place in pure H_2O and D_2O the reactions to be considered are

$$MH_{ads} + MH_{ads} \rightarrow M + H_2 \qquad \text{I}$$

$$MD_{ads} + MD_{ads} \rightarrow M + D_2 \qquad \text{III}$$

The ratio of partition functions is 2 (18). Hence

$$S = 2\ \exp[(1/2(h\nu_o)_{NiH} - 1/2(h\nu_o)_{NiD})]$$

$$= 6 \quad . \tag{173}$$

Results of the derivations presented above for various reaction mechanisms are summarized in Table IV.

Table IV. Theoretical values of separation factors for various reaction mechanisms*

Rate Determining Steps	Isotopic Species / Pure Species	Ratio of Partition Functions	Difference in heats of activation Kcal/mole	Difference in heats of adsorption Kcal/mole	Theoretical Value of S**
Simple Discharge	Isotopic Species	1	1.78		3.0
	Pure H_2 and D_2	1	1.22		7.7
Electrochemical	Isotopic species	1	1.80		6.0
	Pure H_2 and D_2	2	1.535		27.0
Atomic Desorption	Isotopic Species	4/3		0.664	4.0
	Pure H_2 and D_2	2		0.644	6.0

* Calculated from the values of $\Delta\Delta H^{*}_{D-H}$ given by Conway (18).

**Differences in zero point energies in the activated state assumed to be zero.

2.5 Determination of Corrosion Rates from Overpotential Measurements

Stern and Geary (34) showed that for corroding systems controlled by activation polarization a linear relationship is expected in the region where the polarized potential is close to the corrosion potential. For these conditions, the following equation was derived.

$$\left(\frac{\Delta E}{\Delta i}\right)_{E \to o} = \frac{b_c b_a}{(2.3)(i_{corr})(b_c + b_a)} \tag{174}$$

where $\Delta E/\Delta i$ is the polarization resistance, the constants b_c and b_a are the slopes of the logarithmic local cathodic and anodic polarization curves, and i_{corr} is the corrosion current.

Mueller (40) derived the polarization curve of alloys from those of the single metallic components. According to this author the rate of dissolution of an alloy in the active state approaches that of the main metallic component of lowest rate of dissolution within certain limits.

Usually, the conditions in an alloy are complicated as the alloy might not represent a mixture of the crystals of pure metals. Each metal phase might contain a certain percentage of all the metals present or all metals might be contained in a mixed crystal as in the case of stainless steel. If the free energy of the metal components is not essentially changed by alloying, derivation of the polarization curve of the alloy from those of the metallic components might be possible. The condition of the absence of an essential drop of the free energy by alloying is the opposite of that of the validity of Uhlig's electron configuration theory (41), according to which the d-electron vacancies in one of the component metals are filled by electrons originating from some other metallic component or hydrogen. This mechanism would involve a drop of free energy (42).

The conditions of the applicability of Mueller's theory to stainless steels are satisfied, because, according to Evans (42), the free energy of Fe, Cr, and Ni is not essentially changed by alloying to form stainless steels.

On the basis of the above theory, the overall current density of the alloy may be written as

$$i_a = i_x \frac{A_x}{A_a} + i_y \frac{A_y}{A_a} + i_z \frac{A_z}{A_a} \tag{175}$$

where i_a = current density of the alloy

i_x, i_y, i_z = current densities of the single metals X, Y, Z

A_x, A_y, A_z = exposed areas of the metals X, Y, Z

A_a = total exposed area of the alloy

If the concentrations of the single metals on the surface are not different from those in the bulk, the ratio of exposed areas of the single metals to total exposed area of the alloy would equal the ratio of corresponding concentrations of the metals in the alloy to the specific gravity of the respective metals. Hence Eq. (175) can be written as

$$i_a = i_x \frac{C_x}{S_x} + i_y \frac{C_y}{S_y} + i_a \frac{C_z}{S_z} \tag{176}$$

where C_x, C_y, C_z = concentrations of single metals x, y and z expressed in weight per unit volume of the alloy

S_x, S_y, S_z = specific gravity of the single metals X, Y, Z.

The rate at which metal corrodes is proportional to i_{corr}, the corrosion current, defined by (5)

$$E_{corr} = -b \log \frac{i_{corr}}{i_o} \tag{177}$$

where E_{corr} is the corrosion potential (see fig. below).

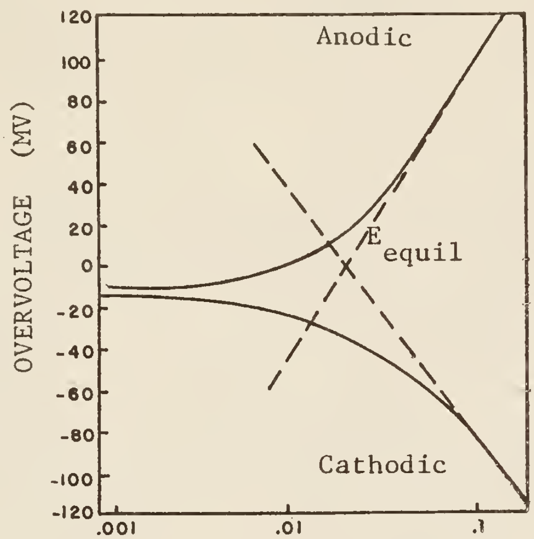

CURRENT DENSITY (Amps/cm^2)

Typical Anodic and Cathodic Polarization Curves for Stainless Steel Showing Corrosion Current as a Function of Potential

Eq. (177) may be used to calculate the corrosion current if b, i_o and the corrosion potential, E_{corr}, are known. The slope b is determined graphically from the Tafel line of the cathodic polarization curve. The exchange current is determined by extrapolation of the Tafel region to the reverse hydrogen potential and the corrosion potential from the cathodic and anodic polarization curves in terms of i_{corr} for alloys as

$$(i_{corr})_a = (i_{corr})_x \frac{C_x}{S_x} + (i_{corr})_y \frac{C_y}{S_y} + (i_{corr})_z \frac{C_z}{S_z} . \tag{178}$$

Eq. (178) indicates that the rate at which an alloy corrodes is given by summing the corrosion rates of individual elements multiplied by its fraction of surface area exposed. This is true for a freshly polished surface. After the corrosion has begun, the situation is much more complex than indicated in Eq. (178), especially in case of passive alloys.

3.0 EXPERIMENTAL

3.1 Description of Equipment

Fig. 4 shows the equipment set-up used to obtain the overvoltage data for HCl in H_2O and DCl in D_2O on stainless steel and nickel electrodes. The system consisted of

A. Electrolytic Cell

B. Hydrogen/Deuterium Purification Unit

C. Water/Heavy Water Purification Unit

A. Electrolytic Cell

The electrolytic cell, shown in Fig. 5 was made of Pyrex glass and was comprised of the following three compartments.

Reference Electrode, I

Cathode, II

Anode, III

I Reference Electrode Compartment (4 cm diam, 12 cm high) consisted of:

2, hydrogen electrode, with 1 cm x 1-1/2 cm platinized platinum electrode, 1.

3, $\mathbb{S}$ 45/50 ground joint cover.

4, water trap, 6 cm long by 2 cm diam.

II Cathode Compartment (6-1/2 cm diam, 22 cm high)

5, test electrodes.

6, thermo-well made of glass for holding a thermometer.

7, $\mathbb{S}$ 29/42 ground glass joint with water seal.

8, $\mathbb{S}$ 71/60 ground glass joint with water seal.

9, four syringe type ground glass joints to provide a leakproof adjustable arrangement.

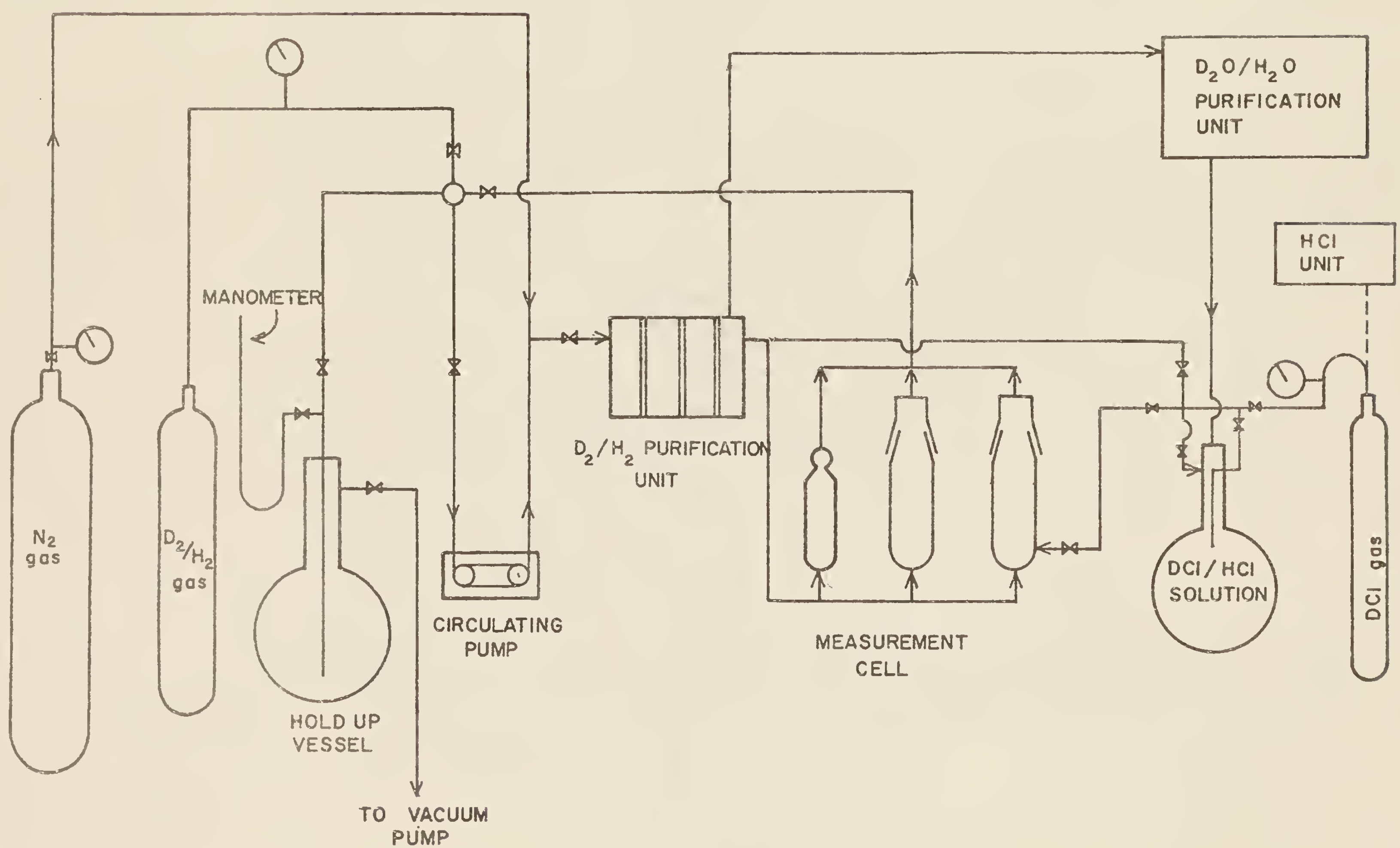

Fig. 4 H_2O/D_2O - SYSTEM

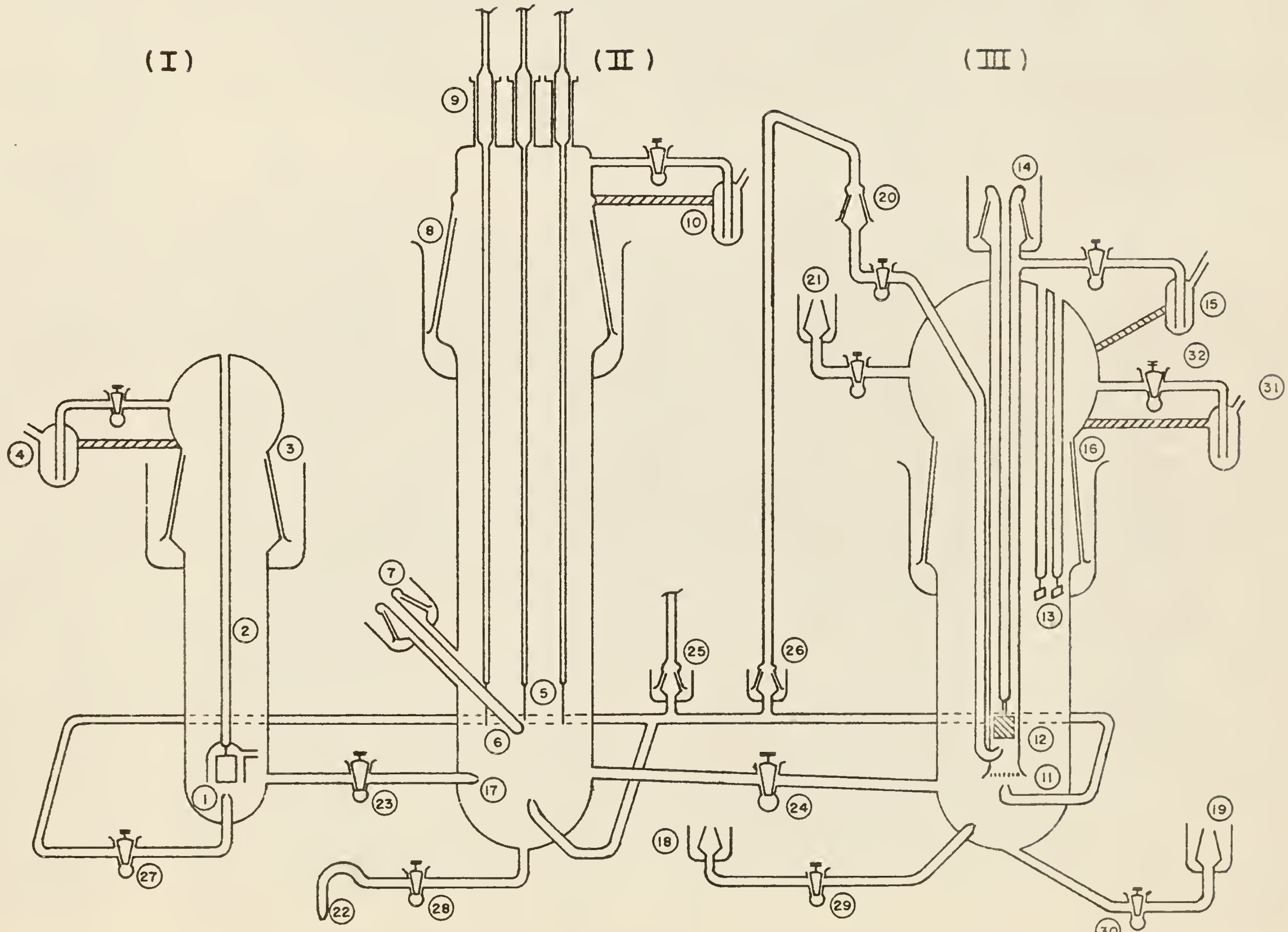

Fig. 5 CELL USED FOR OVERPOTENTIAL MEASUREMENTS.

10, water trap, 6 cm by 2 cm.

III Anode Compartment (6-1/2 cm diam, 22 cm high)

11, fritted glass disk, 1 cm diam, fitted at the bottom of 1-1/2 cm diam tubing which carries the anode.

12, platinized platinum electrode, 1 cm by 1-1/2 cm.

13, two 1 cm by 1 cm platinized platinum electrodes for measurement of conductivity.

14, $ 19/38 ground glass joint with water seal, carries the anode, 12.

15 and 31, water trap, 6 cm by 2 cm.

16, $ 71/60 ground glass joint with water seal.

17, Luggin capillary: a tapered tubing 1-1/2 cm long protruding into the cathode compartment and having 1 mm capillary mouth.

18, $ 10/30 ground glass joint with water seal for transmitting low conductivity water.

19, $ 12/30 ground glass joint on which a trident shaped graphite electrode could be fitted for pre-electrolysis.

20 and 26, $ 10/30 ground glass joints for hydrogen, deuterium or nitrogen supply to the anode.

21, $ 10/30 ground glass joint used as inlet to the anode compartment.

22, drain.

25, main gas inlet $ 10/30 ground glass joint, water seal type.

23, 24, 27, 28, 29, and 30, glass valves.

B. Hydrogen/Deuterium Purification Unit, Fig. 6

Commercial hydrogen gas usually contains trace impurities of oxygen, carbon monoxide, carbon dioxide, hydrocarbons and water vapor. To get rid of these impurities, H_2 was first passed through a series of glass bubblers, each

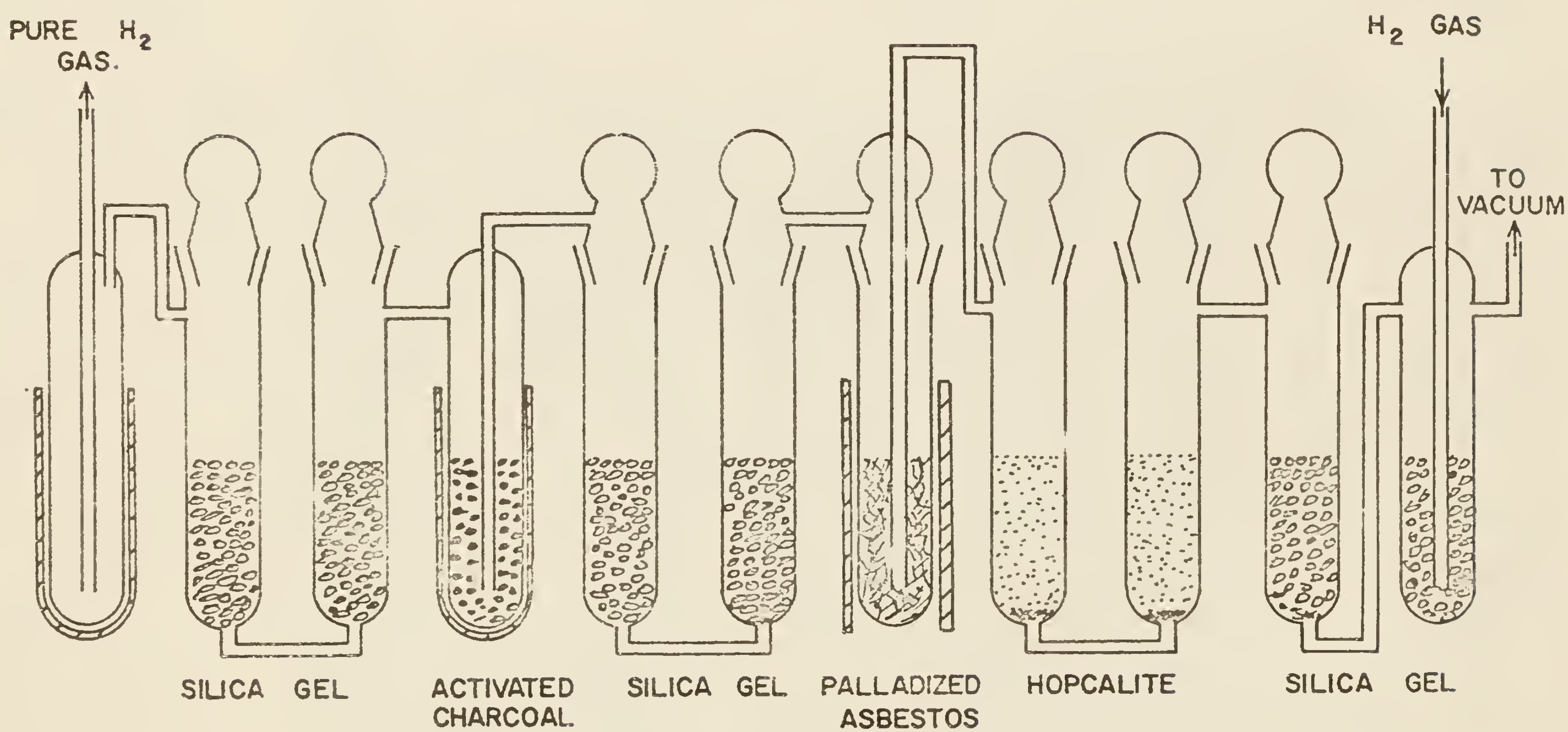

Fig. 6 HYDROGEN PURIFICATION UNIT

approximately 3 cm diam by 16 cm long; the first two containing dry silica gel to remove moisture; the next two containing hopcalite to remove carbon monoxide in absence of moisture. The hydrogen gas was then passed through palladized asbestos (5% Palladium) tube immersed in an electrically heated oven at 500°C to remove oxygen by catalytic combination with hydrogen. Further, bubblers of silica gel were used to remove water produced in the palladium asbestos tube. Four glass traps followed; two containing silica gel and activated charcoal, to remove moisture and some gaseous impurities, and two were kept empty. The last two traps were immersed in dry ice to trap any trace of moisture escaping adsorption by the silica gel.

The same arrangement was used for purification of deuterium gas. All the tubes containing silica gel, hopcalite, palladized asbestos and activated charcoal were dried in the oven at 250°C for about 48 hours to ensure complete removal of moisture.

C. Water Purification Unit

Water used to prepare solutions for electrochemical measurements was purified by redistillation of predistilled water in an all Pyrex glass apparatus. About 60% of the distillate was used. Its specific conductance was 1×10^{-6} mhos/cm. Purified hydrogen gas was passed all the time during distillation. H_2 gas passed was purified according to the method described above.

Electrical Set-Up (Fig. 7)

The electric circuit used consisted of:

1, potentiometer: Type K-3 Universal, Guarded, made by Leeds & Northrup.

2, storage cell: 200 ampere hours; 2 volts.

3, standard cell: Epply unsaturated, internal resistance less than 500 ohms.

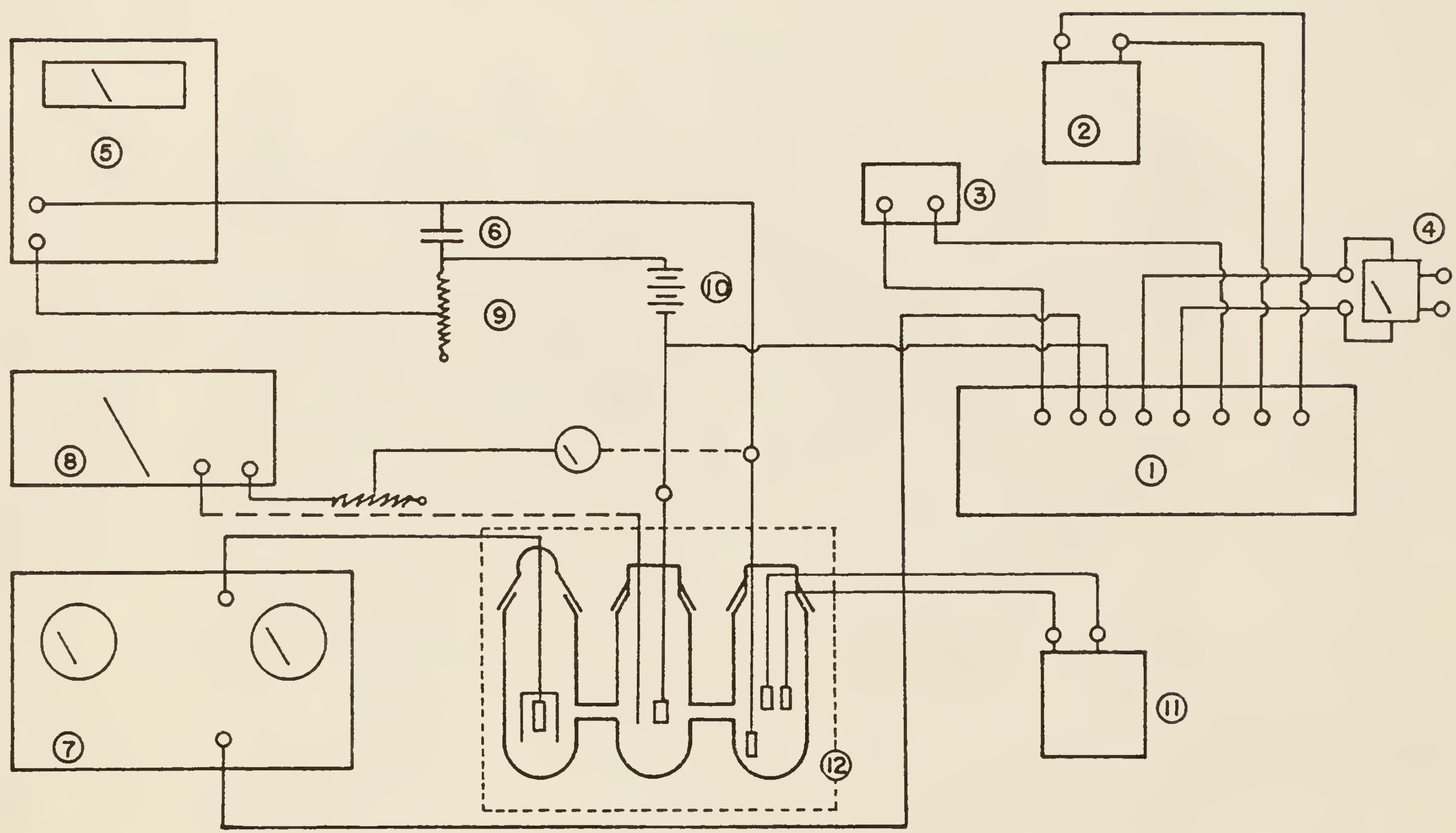

Fig. 7 ELECTRICAL SET UP

4, galvanometer: sensitive reflecting type, used as a null point indicator.

5, electrometer: Keithley Model 600A Electrometer, made by Keithley Instruments; a direct reading ammeter from 3 amperes to 10^{-13} amperes full scale. The current could be measured with an accuracy of 3% of full scale from 3 to 10^{-13} amperes.

6, condenser: 2.5 microfarads, connected in parallel with the input leads of the electrometer. This arrangement avoided the effect of extraneous currents on the measurements.

7, pH-meter: Beckman Model G, used to serve the dual purpose of: (i) measuring the pH of the solution and (ii) acting as a null point indicator for the measurement of potential differences.

8, power supply: Heathkit variable voltage type; used for pre-electrolysis and platinization of electrodes.

9, variable resistance box; 15 ohms to 10 megohms.

10, 6 dry cells, 1.5 volts each.

11, conductivity bridge: Model RC, made by Industrial Instruments.

12, thermostat: for studies on temperature dependence; electronically controlled to keep constant temperatures within ± 0.1°C.

3.2 Techniques

<u>Cathode Preparations</u>

Stainless steel electrodes used as cathodes were of the stainless steel-304 type, 1/16" diam wire, supplied by United Steel Corporation, of known composition (see Appendix B). The sample was already annealed by the suppliers and hence further annealing prior to electrochemical measurements became unnecessary. Each stainless steel cathode consisted of 1-1/4" of the above specimen attached to a short length of 28 SWG Pt by spot welding. The Pt wire was then fused into the Pyrex glass tubing carrying the electrode.

Each electrode was first polished with an emery paper, then electropolished in a solution consisting of 65% by volume H_2SO_4; 22.5% H_2O and 12.5% H_3PO_4. The electrolyte temperature was maintained at 80°C and a current of 50 ma/cm^2 was passed for ten minutes. The electrode was then washed thoroughly with distilled water and immediately fixed in the cathode compartment where pure hydrogen gas atmosphere was maintained.

Nickel cathodes, on the other hand, were made from a spectroscopically pure sample of known analysis supplied by Johnson, Matthey & Co., Ltd.(see Appendix C). Each piece (1 cm x 2 cm, 1/16" thick) was spot welded to Pt and sealed into glass. The Ni cathodes were uniformly polished with emery paper, washed first with acetone and then with conductance water before being fixed in the cathode compartment.

Preparation for Overvoltage Measurements in HCl-H_2O Mixtures

The glass apparatus was cleaned in acid solution, followed by several washings with water of increasing purity. The final washing was done with conductance water and was carried out until the conductivity of the washings was less than 5 x 10^{-6} mhos/cm. The whole system was then assembled, all the traps, joints and valves were sealed with conductance water and the whole system was tested for leakage. The hydrogen purification unit was evacuated and flushed with nitrogen several times to ensure removal of air, in order to avoid explosions. The temperature of the electrical oven surrounding the palladized asbestos tube was maintained between 450°C and 500°C. Air was expelled from the cell by passing a fast current of pure H_2.

A known volume of HCl solution of predetermined concentration, prepared by mixing the appropriate amount of triply distilled azeotropic mixture of $HCl-H_2O$ with conductance water, was then transferred into the anode compartment of the cell. Transfer of conductance water from the distillation apparatus to the mixing flask and of the prepared mixture to the cell were done out of contact of air by applying a pressure of purified H_2 gas. The freshly polished electrode was then transferred into the cathode compartment. The concentration of the HCl solution was checked by measuring the conductivity. The solution was allowed then to be shared between the anode and cathode compartments, the electrode being kept above the level of the solution.

Pre-electrolysing the solution before overvoltage runs was found to be of extreme importance in obtaining reproducible results, as shown below and as also indicated by Bockris (7). For pre-electrolysis the electrical circuit was connected as shown in Fig. 7. The Pt electrode was dipped into the solution and the current adjusted to 10 ma/cm^2. A small current of H_2 gas was allowed to pass into the anode tube to drive out the gasses produced during the period of pre-electrolysis. A period of 15 hours of pre-electrolysis was found sufficient to give reproducible results within the experimental limits. Longer periods of pre-electrolysis did not improve the reproducibility.

At the end of the pre-electrolysis period, the system was ready for the overvoltage measurement. Hydrogen gas was then allowed to pass in the reference electrode compartment for 15 minutes before measurements were started. Overpotential measurements were taken for current densities of zero to 10^{-3} $amps/cm^2$.

Temperature Dependence Measurements

In temperature dependence work the thermostat was adjusted to the appropriate temperature a few hours before the actual measurements were taken to make sure that the inside of the electrolytic cell attained the desired temperature. Temperatures below ambient were obtained by fixing an ice box inside the thermostat. Measurements were taken in this work at 15°, 25°, 35°, 45° and 55°C.

Measurements in $DCl-D_2O$ Mixtures

The general experimental procedure for conducting runs in D_2O solutions was with a few exceptions, very similar to that used for ordinary water solutions. An identical but smaller electrolytic cell was used to conserve as much of D_2O as possible. Deuterium chloride solutions were prepared by bubbling pure DCl gas supplied by Bio-Rad Laboratories through known volume of D_2O. A small amount of the solution was titrated against standard sodium carbonate solution, and a calculated volume of D_2O was added to adjust the solution to the required normality.

D_2 gas was purified in the same manner as H_2. Extreme care was taken to make the system leakproof. At the beginning of each run the whole system was completely flushed with D_2 gas and during the course of the run D_2 gas was circulated between the electrolytic cell and the purification system by a Varistaltic pump to save on the amount consumed.

Special Observations

It should be emphasized here that unless extreme care is taken before and during the runs it would be very difficult to obtain reproducible results. The following points, however, were very helpful in aquiring reproducibility.

1. Long pre-electrolysis to purify the solution from trace impurities. After trying different periods of pre-electrolysis it was concluded that the optimum period was 15 hours for $HCl-H_2O$ and 26 hours for

$DCl-D_2O$ solutions. Longer periods did not improve the results to any noticeable extent.

2. Electropolishing of the electrode surface: Some disagreement between results obtained by different investigations in this field resulted from the irreproducible finishing of electrode surfaces. In this work electropolishing in the solution described above proved to be very effective in that direction.

Although these two points were of very noticeable help yet it should be mentioned that the reproducibility of runs under very identical conditions was still within limits. The statistical approach discussed later in Section 4.1 was, therefore, acquired to take care of this problem.

4.0 RESULTS AND DISCUSSION

4.1 Measurements on Ni Electrodes

As indicated above in Section 3.2 it is difficult to obtain overpotential results unless extreme care is taken in the preparation of solution and electrode surface. To check the results obtained in this work with those obtained by other investigators, work was carried on Ni electrodes in 0.01 N $HCl-H_2O$ and 0.01 N $DCl-D_2O$ solutions which have been previously studied by Bockris (43) and Conway (44). Tables V and VI show typical runs on Ni in 0.01 N $HCl-H_2O$ and 0.01 N $DCl-D_2O$ solutions. Because of the difficulties mentioned above it became necessary to repeat measurements under identical conditions and treat the results statistically as follows.

Tafel slope b and exchange current density i_o were obtained for each η - i_c run by least square fitting of the data in the linear region. An IBM 1410 program was written for this purpose (see Appendix A). Variance of the values of i_o and b obtained from least square fit were calculated by

$$v^2 = \frac{\sum_{i=1}^{N} (x_i - \bar{x})^2}{n - 1} \qquad (179)$$

and for t distribution with (n - 1) degrees of freedom, the values for ± 95% confidence limits, Θ, were calculated from

$$\Theta = t\ v(n)^{1/2}\ . \qquad (180)$$

Values of t were taken from tables in reference (45) at 0.025 probability level for the appropriate number of degrees of freedom.

The statistical curve for Ni in 0.01 N $HCl-H_2O$ solution obtained in this work is shown in Fig. 8 together with the corresponding curve obtained by Bockris (43) under identical conditions. The curves are in fair agreement

Table V. Typical run on Nickel in 0.01 N $HCl-H_2O$ at 25°C, pre-electrolysis for 15 hours

Current Density i/A amps/cm^2	Potential Difference ΔV volts	Overpotential η volts
0	+0.141	+0.023
4.80×10^{-7}	+0.0830	-0.035
5.70×10^{-7}	+0.0770	-0.041
9.44×10^{-7}	+0.0600	-0.058
1.37×10^{-6}	+0.0460	-0.072
1.94×10^{-6}	+0.0300	-0.088
2.92×10^{-6}	+0.0140	-0.104
4.57×10^{-6}	-0.0040	-0.122
6.29×10^{-6}	-0.0260	-0.144
9.15×10^{-6}	-0.0370	-0.155
1.26×10^{-5}	-0.0520	-0.170
1.77×10^{-5}	-0.0670	-0.185
2.52×10^{-5}	-0.0790	-0.195
3.77×10^{-5}	-0.0950	-0.213
5.14×10^{-5}	-0.1130	-0.231
6.86×10^{-5}	-0.1320	-0.250

Table VI. Typical run on Nickel in 0.01 N $DCl-D_2O$ at 25°C, pre-electrolysis for 26 hours

Current Density i/A amps/cm^2	Potential Difference ΔV volts	Overpotential η volts
0	+0.2366	+0.0952
8.20×10^{-7}	+0.0314	-0.1100
1.00×10^{-6}	+0.0212	-0.1202
1.55×10^{-6}	-0.0011	-0.1425
2.32×10^{-6}	-0.0238	-0.1652
3.30×10^{-6}	-0.0336	-0.1750
5.00×10^{-6}	-0.0609	-0.2023
7.80×10^{-6}	-0.0769	-0.2183
1.15×10^{-5}	-0.1009	-0.2423
1.52×10^{-5}	-0.1106	-0.2521
2.30×10^{-5}	-0.1365	-0.2779
3.30×10^{-5}	-0.1455	-0.2869
4.40×10^{-5}	-0.1681	-0.3105
6.60×10^{-5}	-0.1809	-0.3223
9.00×10^{-5}	-0.1968	-0.3382
1.15×10^{-4}	-0.2138	-0.3552
1.52×10^{-4}	-0.2286	-0.3700
2.25×10^{-4}	-0.2418	-0.3832

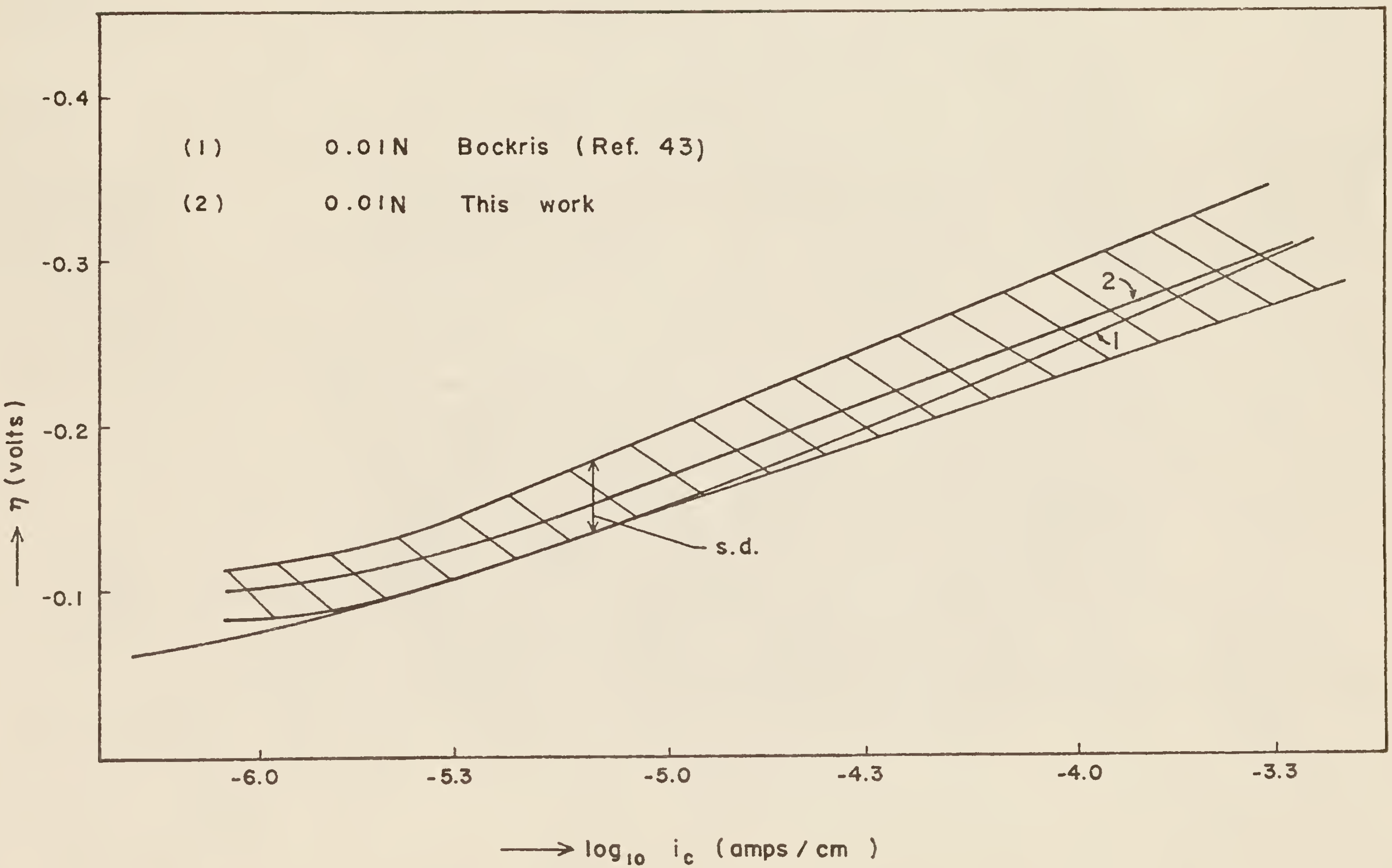

Fig. 8 STATISTICAL TAFEL LINES FOR CATHODIC POLARIZATION OF NICKEL IN $HCl - H_2O$ SOLUTIONS.

with each other. Fig. 9 shows the statistical Tafel lines in 0.01 N $HCl-H_2O$ and 0.01 N $DCl-D_2O$ solutions at 25°C. The shaded area around the statistical line is determined by taking the standard deviation, σ, given by

$$\sigma_{.} = \pm\left[\frac{\sum_{n=1}^{n}(x_i - \bar{x})^2}{n}\right]^{1/2} \qquad (181)$$

where x_i's are the overpotential values for a fixed current density for all the Tafel lines under consideration and $\bar{x}$ is the mean of these values. Results obtained on stainless steel were treated statistically in the same way.

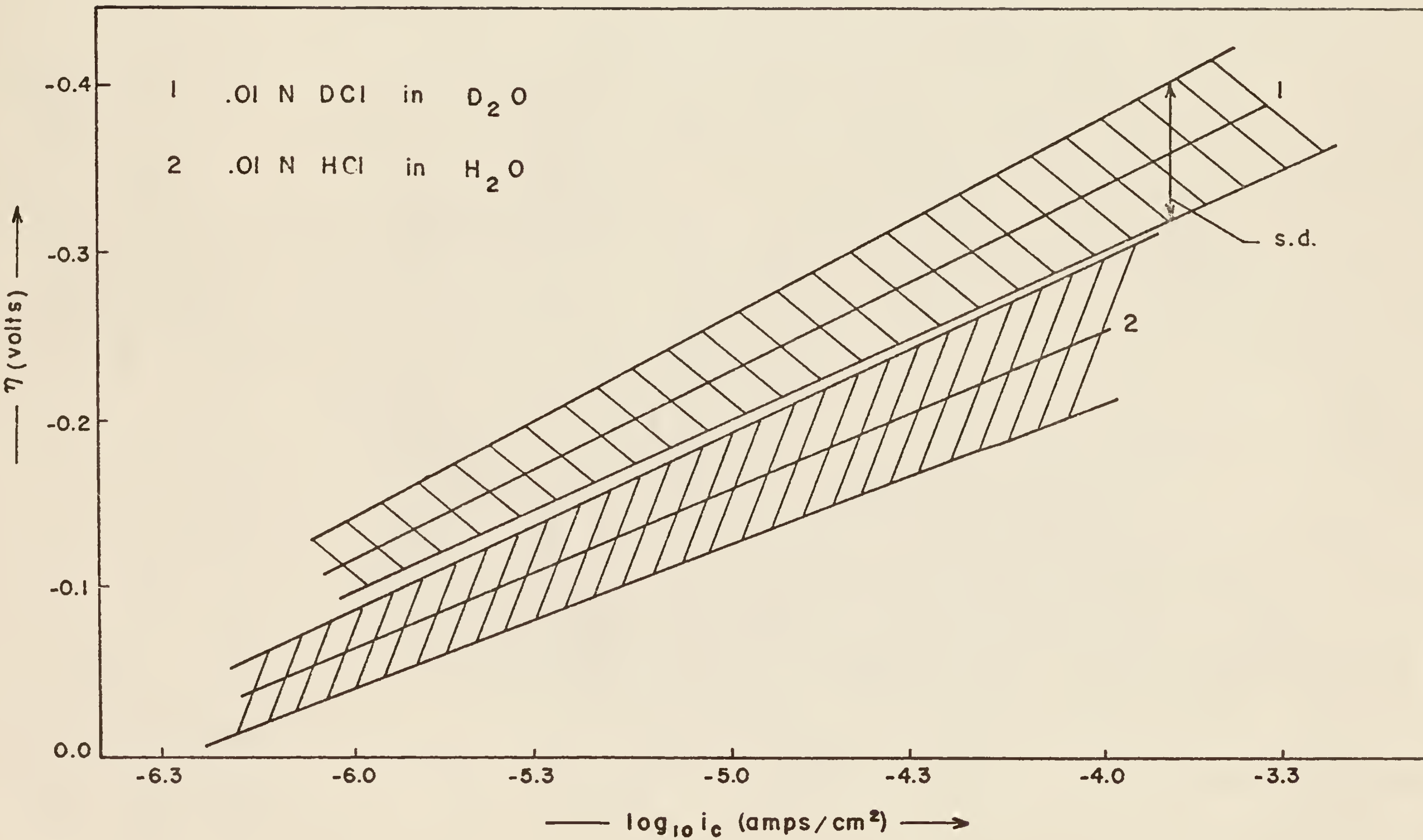

Fig. 9 STATISTICAL TAFEL LINES FOR CATHODIC POLARIZATION OF NICKEL IN 0.01 N HCl (in H_2O) AND 0.01 N DCl (IN D_2O) AT 25° C.

4.2 Measurements on Stainless Steel Electrodes

4.2.1 Tafel Slopes and Stoichiometric Number, μ

Typical measurements of overpotential at various cathodic current densities made on stainless steel electrode in HCl and DCl solutions are presented in Tables VII and VIII. Figs. 10 and 12 show plots of typical runs in HCl and DCl solutions on stainless steel with and without pre-electrolysis. There is a good amount of departure from linearity of Tafel curves for hydrogen and deuterium runs in case of insufficient solution purity. This showed clearly the remarkable effect of pre-electrolysis on the data obtained. The Tafel curves in such impure solutions showed two slopes, one at lower current densities and the other at higher current densities. The same phenomena has been observed by Bockris (7) and others in presence of impurities. Even with pre-electrolysis, a small time variation in the electrode potential was observed and the most reproducible results were obtained when the Tafel line was established by the rapid technique (7), i.e., by taking the measurements with minimum possible delay as soon as steady electrode potential was indicated by the null galvanometer.

In all the Tafel lines two non-linear regions, one at low current densities and another at high current densities, existed. Fig. 13 shows the statistical Tafel lines for stainless steel electrodes in $HCl-H_2O$ solutions of different pH values between 0.2 and 3.8. Table IX gives the corresponding values of b and log i_o. The ± 95% confidence limits on these values were calculated by the method mentioned above. As seen from Table IX no dependence of the Tafel slopes on pH was observed indicating that the reaction mechanism did not change with the change in pH. The variation of log i_o and η with pH is shown in Figs. 14 and 15.

Table VII. Typical run on stainless steel-304 in 0.01 N $HCl-H_2O$ solution at 25°C, pre-electrolysis for 15 hours

Current density i/A amps/cm^2	Potential Difference ΔV volts	Overpotential η volts
0	+0.1974	+0.0584
8.30×10^{-7}	+0.0035	-0.1145
1.00×10^{-6}	-0.0020	-0.1200
1.65×10^{-6}	-0.0260	-0.1440
2.40×10^{-6}	-0.0685	-0.1665
3.40×10^{-6}	-0.0680	-0.1860
5.20×10^{-6}	-0.1020	-0.2200
8.05×10^{-6}	-0.1176	-0.2356
1.15×10^{-5}	-0.1370	-0.2550
1.65×10^{-5}	-0.1592	-0.2772
2.30×10^{-5}	-0.1780	-0.2960
3.50×10^{-5}	-0.2023	-0.3203
4.90×10^{-5}	-0.2208	-0.3388
7.85×10^{-5}	-0.2482	-0.3662
1.10×10^{-4}	-0.2670	-0.3850
1.75×10^{-4}	-0.2940	-0.4120
2.30×10^{-4}	-0.3106	-0.4286
3.60×10^{-4}	-0.3470	-0.4650
4.90×10^{-4}	-0.3540	-0.4720

Table VIII. Typical run on stainless steel-304 in 0.01 N $DCl-D_2O$ at 25°C, pre-electrolysis for 26 hours

Current Density i/A amps/cm^2	Potential Difference ΔV volts	Overpotential η volts
0	+0.2085	+0.067
8.10×10^{-7}	-0.0565	-0.198
1.00×10^{-6}	-0.0585	-0.200
1.65×10^{-6}	-0.0765	-0.218
2.40×10^{-6}	-0.0975	-0.239
3.40×10^{-6}	-0.1185	-0.260
5.10×10^{-6}	-0.1455	-0.287
7.95×10^{-6}	-0.1715	-0.313
1.10×10^{-5}	-0.1915	-0.333
1.65×10^{-5}	-0.2185	-0.360
2.30×10^{-5}	-0.2385	-0.380
3.40×10^{-5}	-0.2655	-0.407
4.80×10^{-5}	-0.2865	-0.428
7.65×10^{-5}	-0.3085	-0.450
1.10×10^{-4}	-0.3385	-0.480
1.60×10^{-4}	-0.3615	-0.503

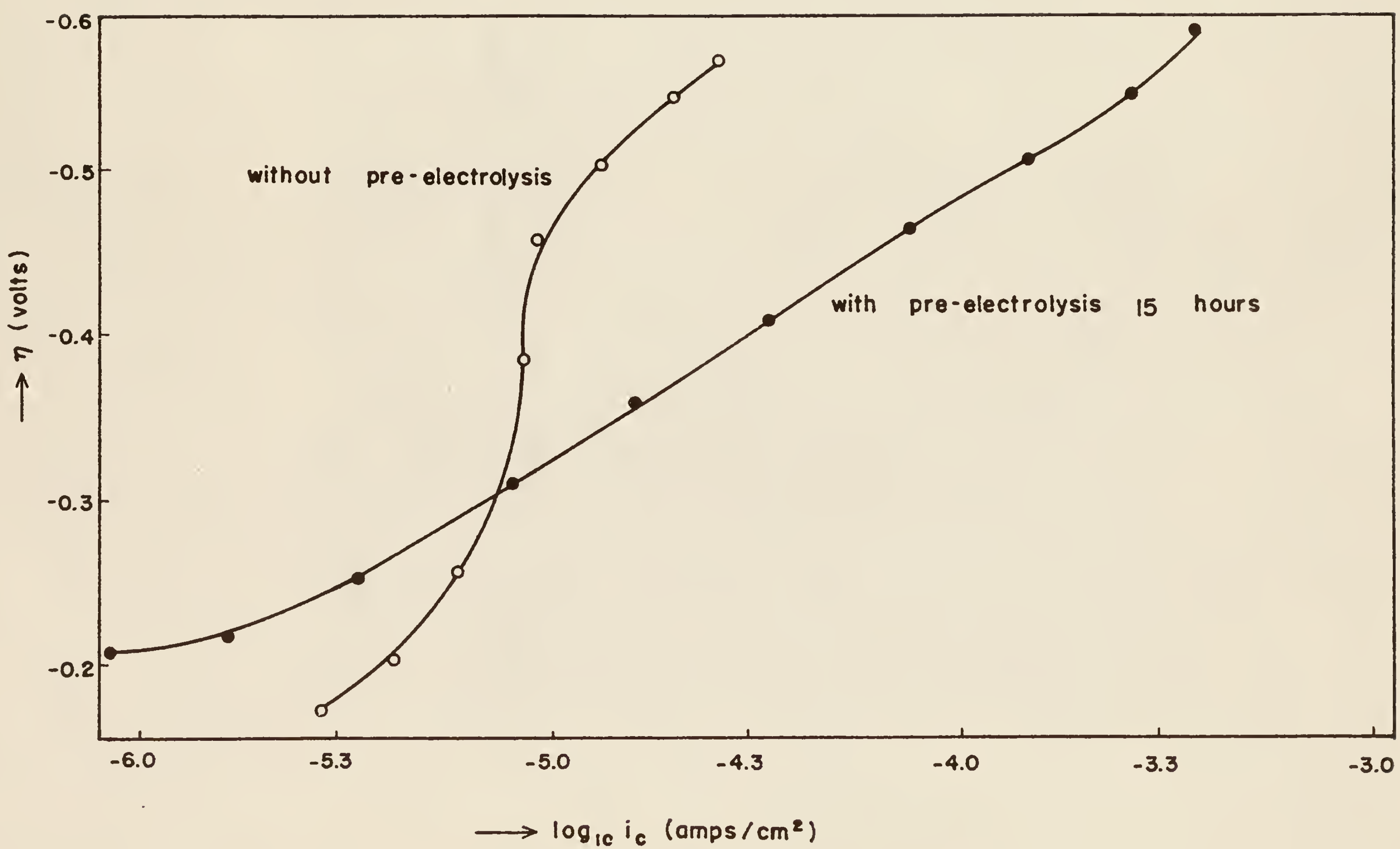

Fig. 10 TYPICAL TAFEL LINES FOR CATHODIC POLARIZATION OF STAINLESS STEEL -304 IN .01 N HCl (in H_2O) SHOWING THE EFFECT OF PRE-ELECTROLYSIS

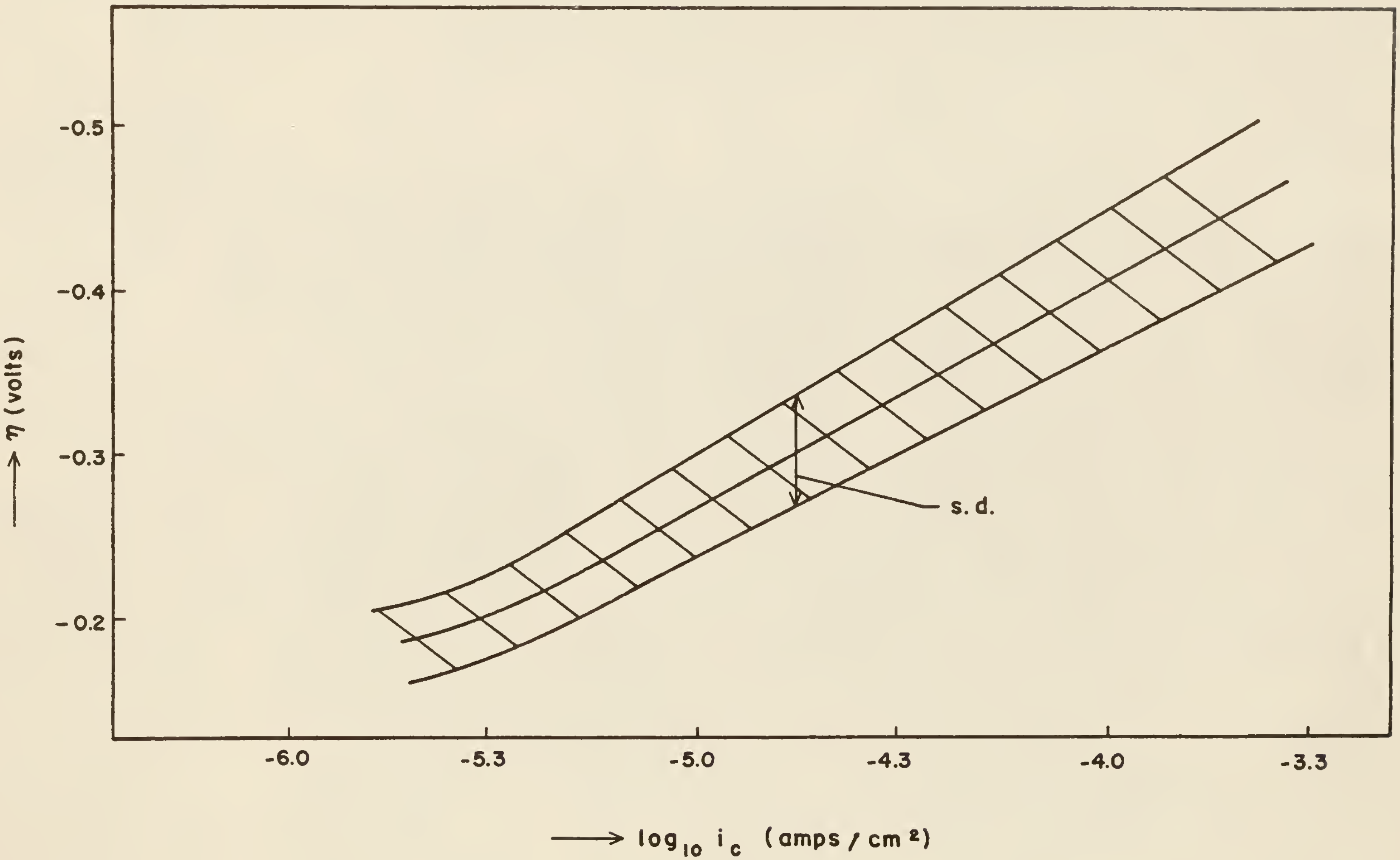

Fig. 11 STATISTICAL TAFEL LINE FOR CATHODIC POLARIZATION OF S.S. -304 IN 0.01 N HCl (in H_2O)

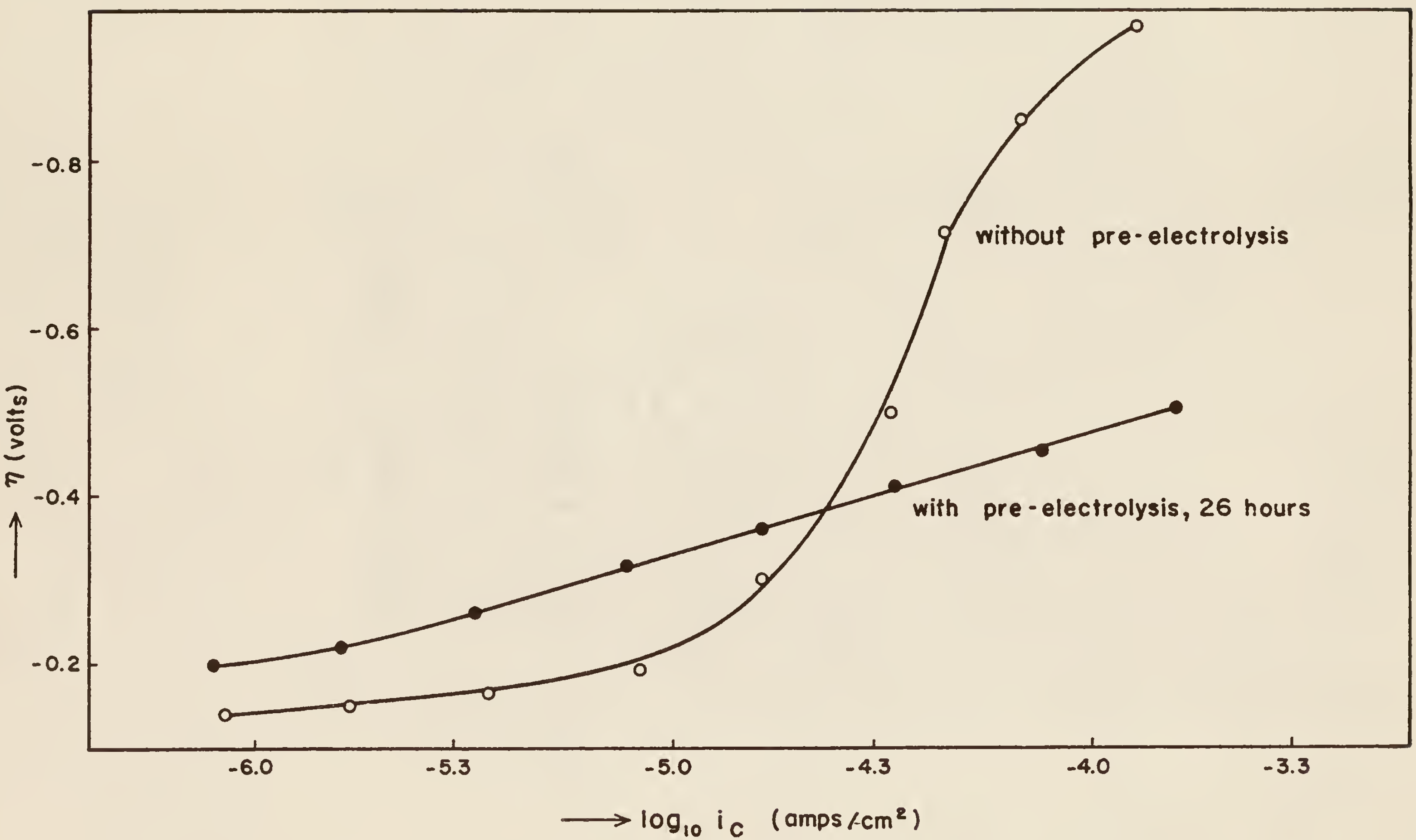

Fig. 12 TYPICAL TAFEL LINES FOR CATHODIC POLARIZATION OF STAINLESS STEEL-304 IN .01 N DCl (IN D_2O) SHOWING THE EFFECT OF PRE-ELECTROLYSIS

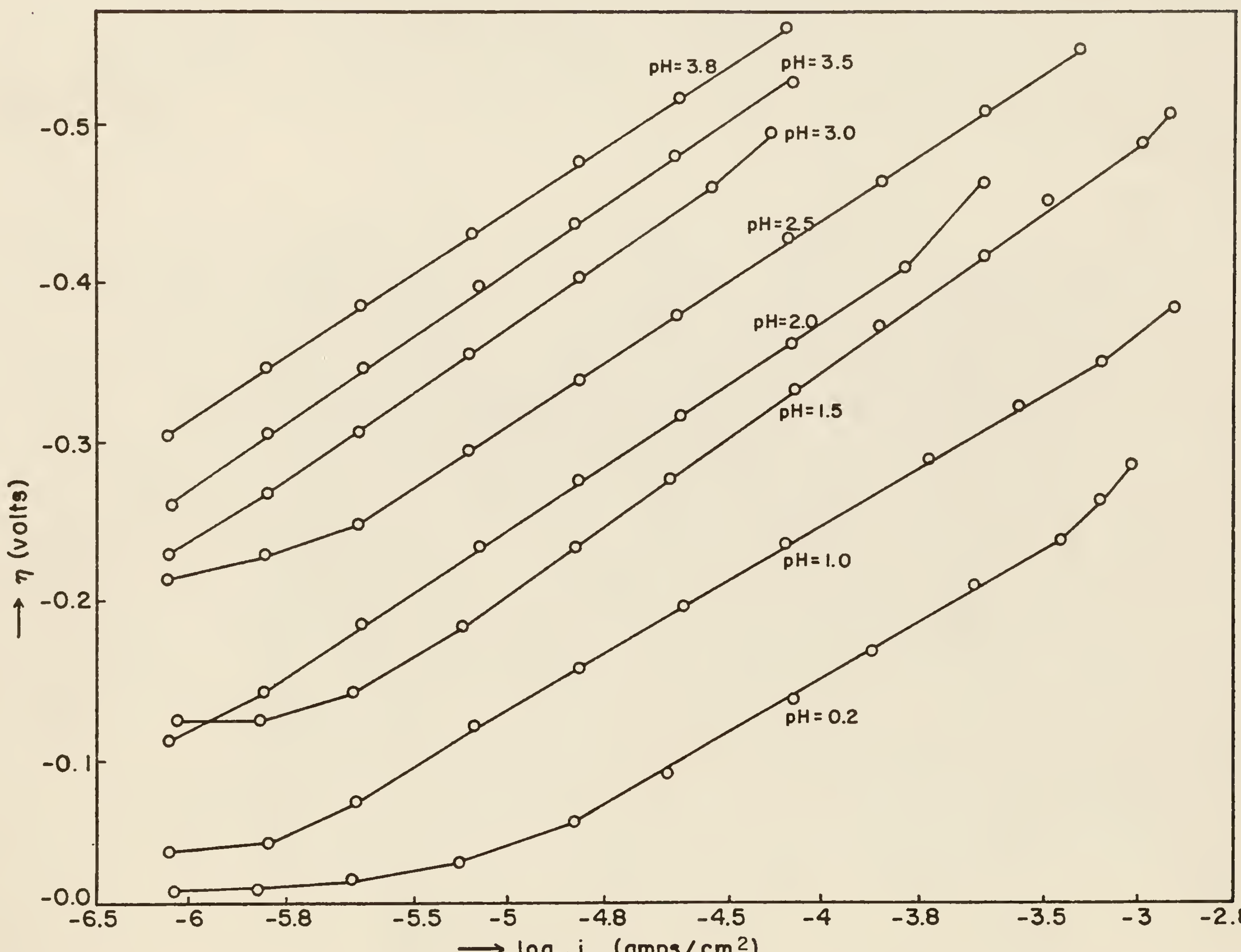

Fig.13 Effect of pH on cathodic polarization of stainless steel-304 in HCl - H_2O solutions

Table IX. Statistically computed average Tafel lines and derived data for stainless steel cathodes in $HCl-H_2O$ solutions at 25°C

pH	n	a	b	95% limits of b	$-\log i_o$	95% limits of $\log i_o$
.2	4	0.6542	0.05367	±0.001	5.294	±0.10
1.0	5	0.8160	0.05843	±0.012	6.052	±0.08
1.5	7	0.8907	0.06108	±0.010	6.324	±0.10
2.0	5	0.9787	0.06103	±0.005	6.965	±0.14
2.5	7	0.9591	0.05713	±0.005	7.295	±0.08
3.0	5	1.0944	0.06074	±0.013	7.792	±0.38
3.5	6	1.1161	0.06017	±0.012	8.060	±0.19
3.8	5	1.1641	0.06081	±0.015	8.309	±0.19

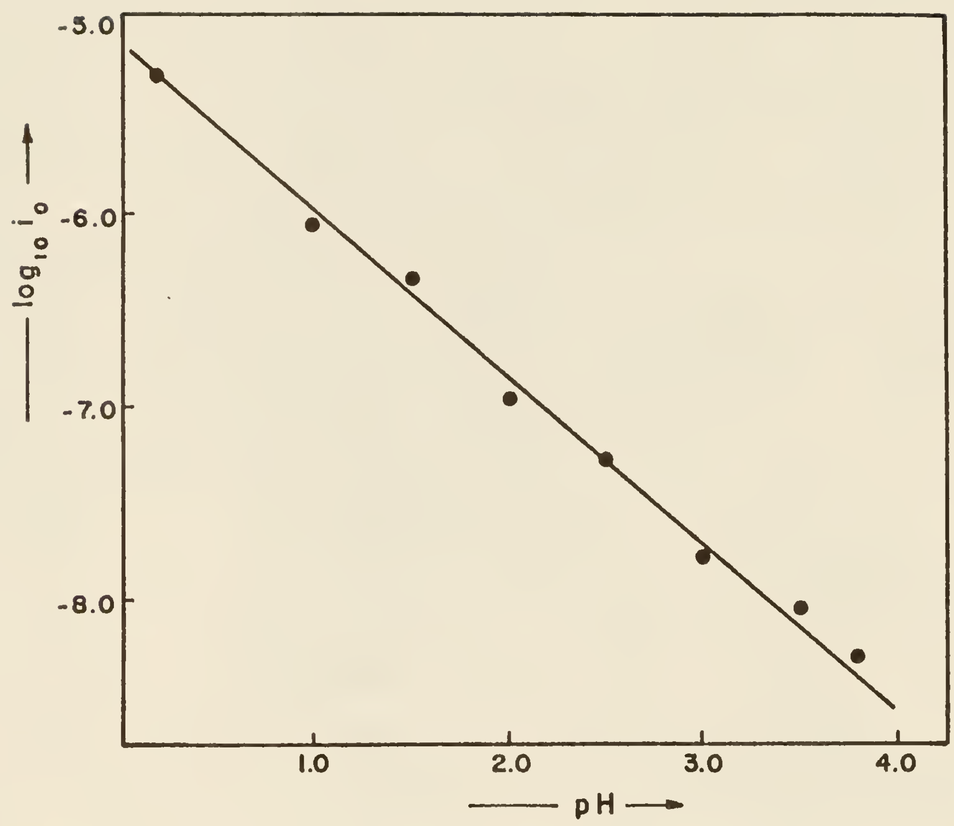

Fig. 14 VARIATION OF $\log_{10} i_o$ WITH pH

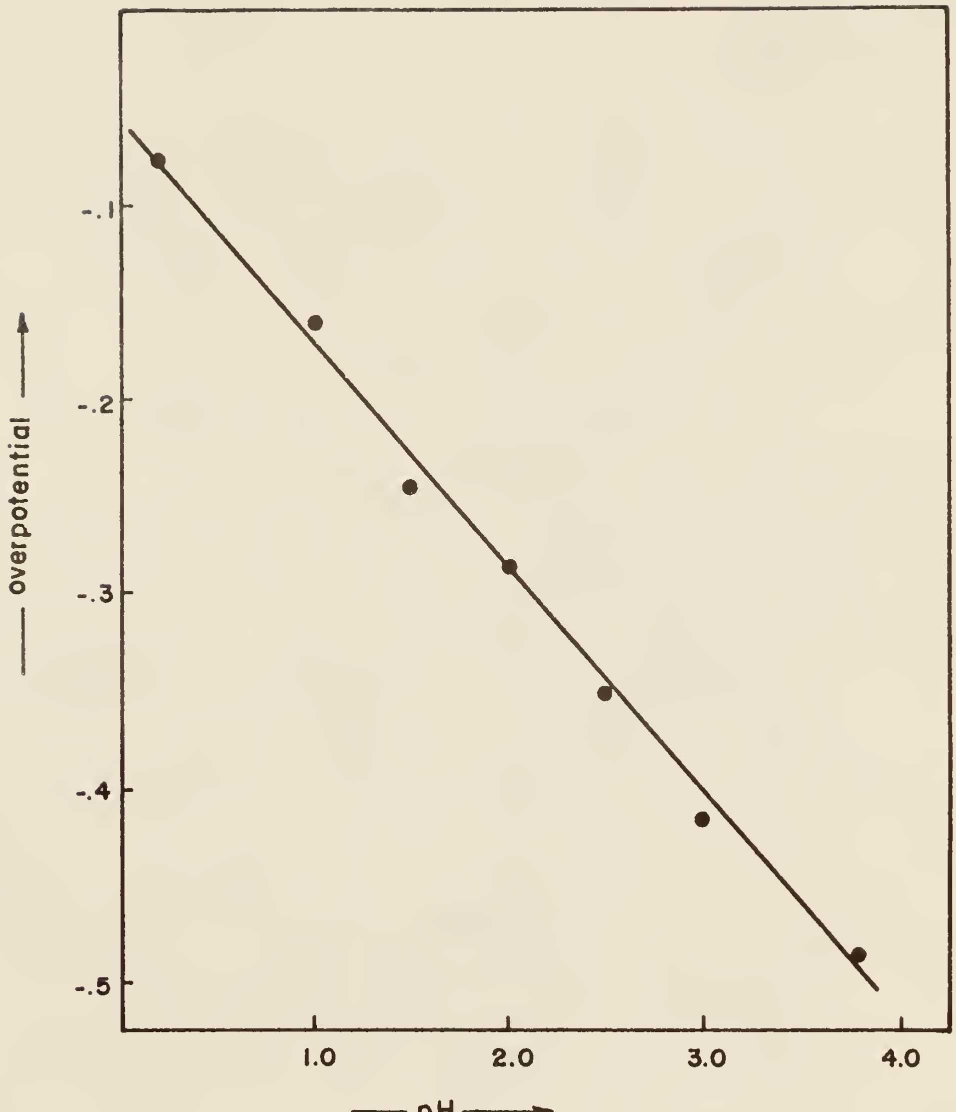

Fig. 15 VARIATION OF OVERPOTENTIAL (at $\log_{10} i_c = -4.8$) WITH pH.

Table X gives the values of b and i_o for stainless steel in H_2O and D_2O solutions. It is obvious that b is almost the same in the two cases, indicating that there is no change in the reaction mechanism due to deuterium substitution. It is also observed that these values of b and those recorded in Table IX were always above 0.051. Comparison of experimental values of b with the corresponding theoretically calculated values given in Table XI (44) shows that the rate determining step in the reaction mechanism on the stainless steel surface is either simple discharge or electrochemical desorption. It has been established that the rate determining mechanism on Fe is simple discharge (44) and that on Ni is electrochemical desorption (43) both of which have theoretical b values of 0.051 (Table XI). Assuming that each of the three elements, Fe, Ni, and Cr composing the stainless steel alloy will keep its individuality as indicated in Section 2.5, it can be concluded that the rate determining step in hydrogen/deuterium evolution on Cr is either simple discharge or electrochemical desorption. To the best of author's knowledge no direct study of hydrogen evolution on Cr electrode surfaces has been made because of its high reactivity.

Table XII includes values of the stoichiometric number, μ, defined by Eq. (107)

$$\mu = \frac{-2\ i_o F}{RT} (d\eta/d\ i_c)_{\eta \to o} \tag{107}$$

$(d\eta/d\ i_c)_{\eta \to o}$, the slope of the non-linear part of η - i_c curve, is rather difficult to measure, since it gradually varies and could give rise to indefinite values of μ. Generally speaking it is very difficult to measure the value of μ in acid solutions due to slight dissolution of the electrode which occurs at low current densities. As seen in Table XII, values of μ vary between 0.84 and 2.12 with an average value of μ = 1.51. This is also

Table X. Statistical values of i_o and b in $HCl-H_2O$ and $DCl-D_2O$ solutions at 25°C

Solution	Normality	Temperature	i_o	b	r
$HCl-H_2O$	0.01	25°C	1.1019×10^{-7}	0.06103	2.54
$DCl-D_2O$	0.01	25°C	4.3484×10^{-8}	0.06377	

Table XI. Theoretical values of μ and b for various mechanisms of cathodic hydrogen evolution in acid solutions

Mechanism	$b = \frac{RT}{F}$	Numerical Value of b	μ
Slow Discharge Fast Atomic Desorption (A)	2RT/F	0.0512	2
Slow Atomic Desorption Fast Discharge (B)	RT/2F	0.0128	2
Slow Discharge Fast Electrochemical (C)	2RT/F	0.0512	2
Slow Electrochemical	2RT/3F	0.0171	1
Fast Discharge (D)	2RT/F	0.0512	1

Table XII. Typical values of the stoichiometric number, μ, in HCl-H_2O solutions of various pH at 25°C

pH	i_o amps/cm^2	non-linear slope at $\eta \to o$	μ
0.2	4.286×10^{-6}	5.06×10^{3}	1.69
0.2	5.985×10^{-6}	3.24×10^{3}	1.51
0.2	5.664×10^{-6}	4.81×10^{3}	2.12
1.0	1.190×10^{-6}	1.57×10^{4}	1.45
1.0	0.967×10^{-6}	2.12×10^{4}	1.60
1.0	0.905×10^{-6}	2.59×10^{4}	1.82
1.5	0.312×10^{-6}	5.90×10^{4}	1.43
1.5	0.554×10^{-6}	3.51×10^{4}	1.51
1.5	0.384×10^{-6}	5.70×10^{4}	1.70
2.0	0.759×10^{-7}	2.23×10^{5}	1.32
2.0	1.507×10^{-7}	1.39×10^{5}	1.63
2.0	0.954×10^{-7}	1.13×10^{5}	0.84
2.5	0.536×10^{-7}	2.25×10^{5}	0.94
2.5	0.657×10^{-7}	2.89×10^{5}	1.48
2.5	0.383×10^{-7}	5.34×10^{5}	1.59

the most probable value. Comparison of these values with the theoretically calculated values of μ shown in Table XII does not lead to a definite conclusion regarding the rate determining step in the reaction mechanism. It does, however, favor the above conclusions arrived at by comparing the experimental and theoretical values of the Tafel slopes.

4.2.2 Isotopic Ratio and Surface Coverage

Fig. 16 shows the statistical Tafel lines of stainless steel in 0.01 N $HCl-H_2O$ and 0.01 N $DCl-D_2O$ solutions. Values of the exchange current densities and the isotopic ratio, R, defined as

$$R = (i_o)_{H_2O} / (i_o)_{D_2O} \tag{182}$$

are given in Table X. R has been found to be characteristic of the rate determining step in the mechanism of the hydrogen/deuterium evolution reaction (44).

Surface coverage, defined as the fraction of the surface covered with hydrogen/deuterium atoms may affect the isotopic ratio, R. Surface coverage effects can arise from: (a) differences in the steady-state surface concentrations of adsorbed H or D in the rate determining step, and (b) the dependence of heats of adsorption of H and D on coverage. It has been shown by Conway (18) that effects of type (a) are small, particularly for highly covered surfaces. Experimentally (46) at smooth platinum, surface coverage by adsorbed D is about 15 to 20% greater, at a given potential, than that by H. In this case the rate of the electrochemical and atom desorption reactions would tend to be slightly greater for D entities than for H entities were it not for the large opposite effect of zero point energy differences. Effects of type (b) can be much larger than those of type (a). Conway (44) found that if simple discharge were rate determining the value of R would be

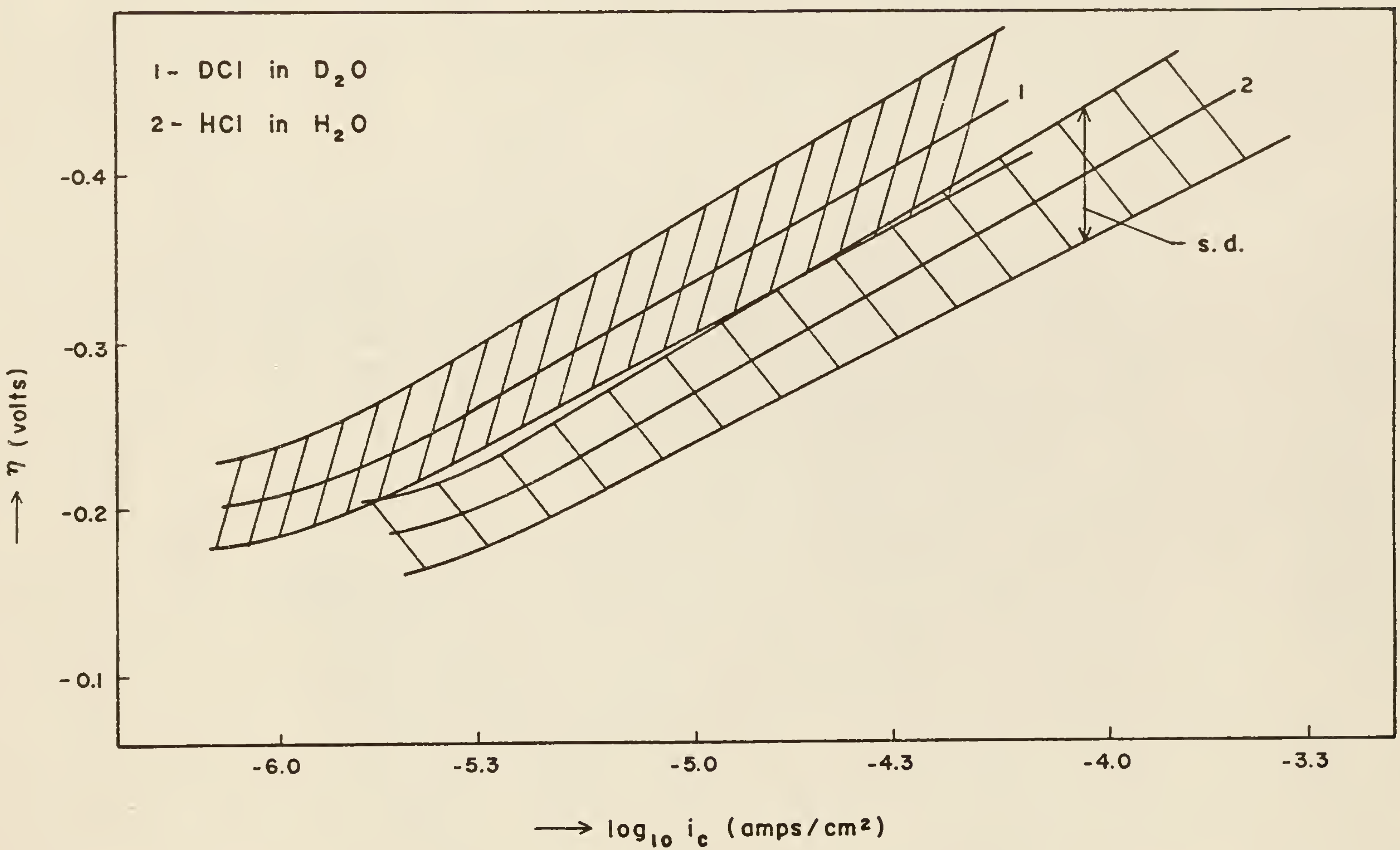

Fig. 16 STATISTICAL TAFEL LINES FOR CATHODIC POLARIZATION OF S.S. -304 IN 0.01 N HCl (in H_2O) AND 0.01 N DCl (in D_2O).

independent of surface coverage while in case of electrochemical desorption surface coverage will have a direct effect on R. On the basis of the values of R recorded in Table XIII and on the assumption that the overall value of R in case of stainless steel is the sum of the partial contributions of Fe, Cr and Ni and that alloying does not change the rate determining step of individual elements, the following analysis can be presented.

Considering the rate determining steps on Fe and Ni as simple discharge (47), and electtrochemical desorption (44), respectively, and that on Cr as either simple discharge or electrochemical desorption, as indicated above from the experimental value of the Tafel slope, b, the experimental value of R can be used to identify the rate determining step on Cr by calculating the theoretical values of R for the two cases: (i) when rate determining step on Cr is a simple discharge and (ii) when the rate determining step on Cr is electrochemical desorption and comparing the values obtained with the experimental value. Table XIV shows the values of R calculated for the above two cases. Comparing the experimental value of R = 2.54 determined in this work and recorded in Table X with the values in Table XIV it can be concluded that the rate determining step of the hydrogen/deuterium evolution reaction on Cr is simple discharge.

4.2.3 Difference in Heats of Activation and the Limiting Value of the Separation Factor, S

As indicated in Section 2.4.2 the separation factor, S, can be determined from

$$S = (C_D/C_H)_I \frac{\pi_a(\text{H reactants})\ [F^\circ_H/\pi_f(\text{H reactants})]}{\pi_a(\text{D reactants})\ [F^\circ_D/\pi_f(\text{D reactants})]} \exp[(\Delta H^*_{o,D} - \Delta H^*_{o,H})/RT] \ . \tag{135}$$

Table XIII. Isotopic ratios, R, of exchange currents for various mechanisms

Mechanism	Surface Coverage, 0	0.5	0.75	1
Simple Discharge	2.2	2.2	2.2	2.2
Electrochemical	9.6	6.8	6.0	5.6
Atom Desorption	18.0	6.0	3.5	2.0

Table XIV. Theoretical values of R for stainless steel for Cases (i) and (ii)*

Case	Surface Coverage	Contribution to R from the component: Fe	Ni	Cr	R
(i)	1.00	1.628	.448	.397	2.473
	0.75	1.628	.48	.397	2.525
	0.50	1.628	.544	.397	2.569
	0	1.628	.767	.397	2.792
(ii)	1.00	1.628	.448	1.009	3.085
	0.75	1.628	.48	1.08	3.188
	0.50	1.628	.544	1.222	3.394
	0	1.628	.767	1.73	4.125

*Calculated from Table XIII.

If the rate determining step in hydrogen/deuterium evolution is simple discharge and the measurements made on pure $HCl-H_2O$ and $DCl-D_2O$ solution of same acidic concentration

$$(C_D/C_H)_I = 1$$

$$\frac{\pi_a(\text{H reactants})}{\pi_a(\text{D reactants})} = 1$$

$$\frac{[F_H^\circ/\pi_f(\text{H reactants})]}{[F_D^\circ/\pi_f(\text{D reactants})]} = 1$$

and Eq. (135) reduces to

$$S = \exp[(\Delta H_D^* - \Delta H_H^*)/RT] \quad (183)$$

where ΔH_H^* and ΔH_D^* are the heats of activation of hydrogen and deuterium reactions respectively. S can be directly found from the above equation if $\Delta\Delta H^*_{D-H} = \Delta H_D^* - \Delta H_H^*$ is evaluated theoretically or determined experimentally. Values of ΔH_D^* and ΔH_H^* were determined experimentally in this investigation on stainless steel at different temperatures in 0.01 N $HCl-H_2O$ (Fig. 17) and 0.01 N $DCl-D_2O$ solution (Fig. 18) by using the relation

$$\log i_o = \log B - \Delta H^*/2.303\ RT \quad (184)$$

where B is known as the Eyring's entropy function (43). The statistical values of i_o and b obtained at different temperatures are presented in Table XV. As seen in the table, there is no appreciable change in Tafel slope due to change in temperature indicating that the reaction mechanism is independent of temperature. Figs. 19 and 20 show the values of $\log i_o$ versus $\frac{1}{T}$ obtained in 0.01 N $HCl-H_2O$ and 0.01 N $DCl-D_2O$ respectively. The points on the plot were subjected to least squares analysis using $\frac{1}{T}$ as the independent variable. Table XVI shows the slopes obtained, values of ΔH^* computed from the slopes,

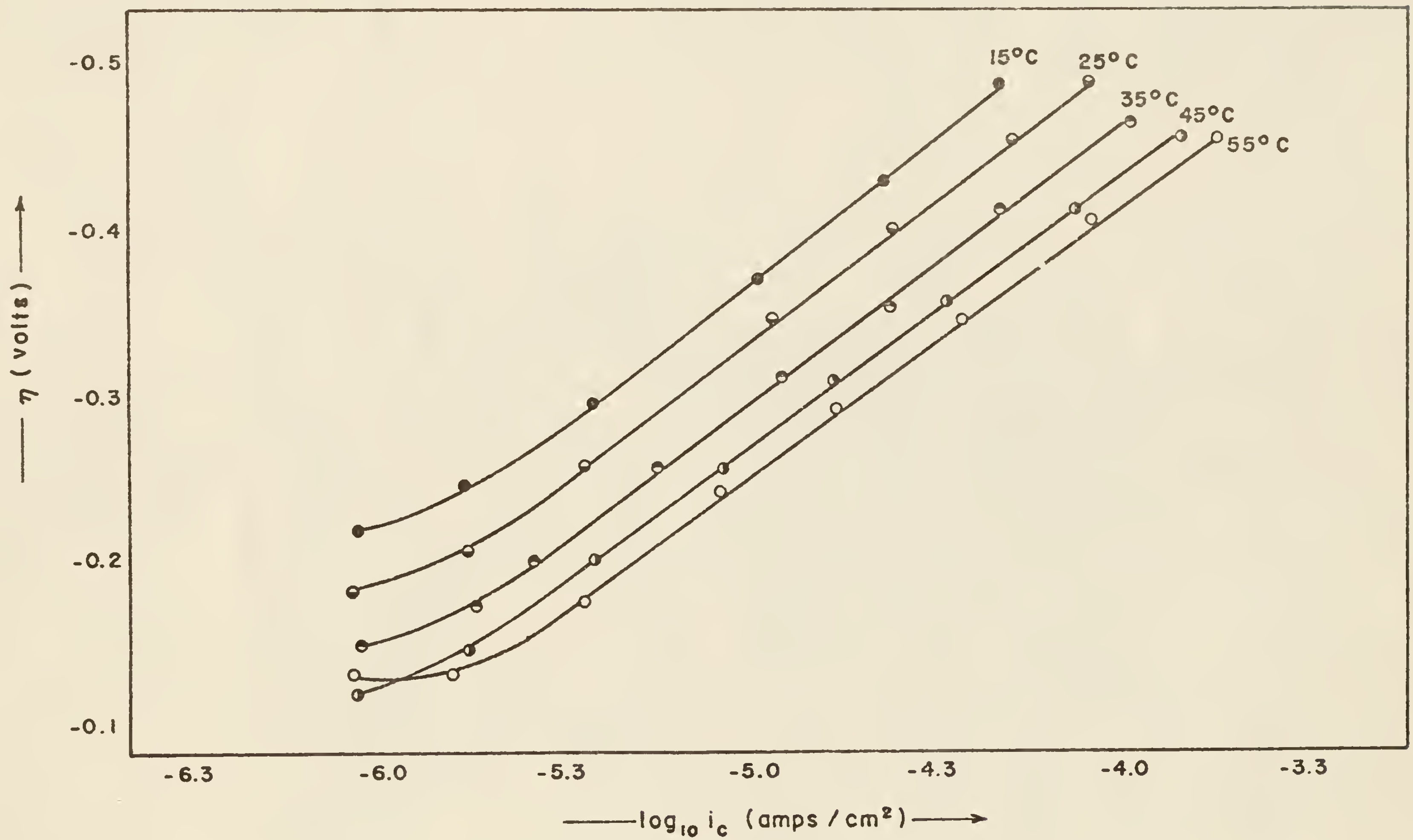

Fig. 17 TAFEL LINES FOR CATHODIC POLARIZATION OF S.S.-304 IN 0.01 N HCl - H_2O SOLUTION AT DIFFERENT TEMPERATURES.

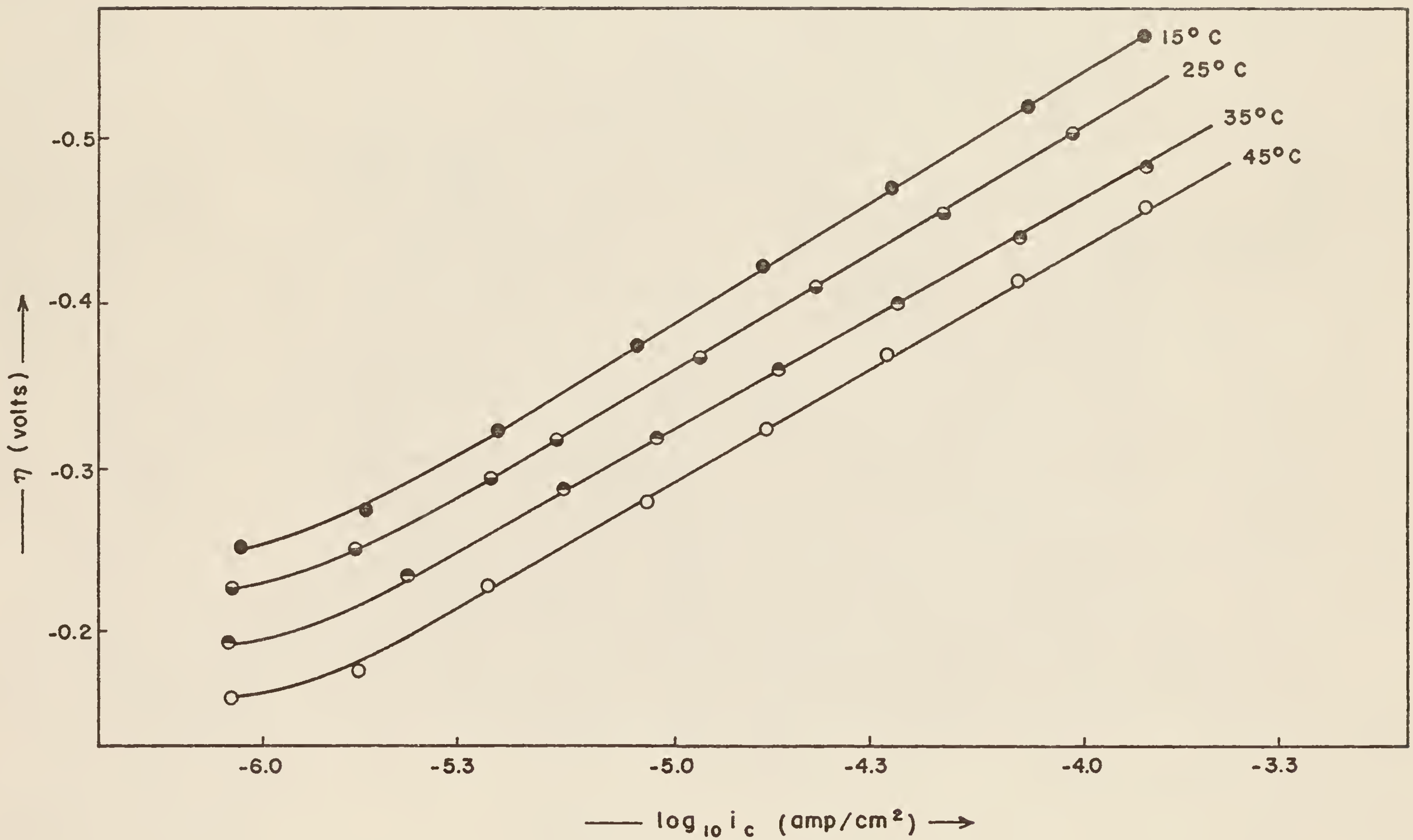

Fig. 18 TAFEL LINES FOR CATHODIC POLARIZATION OF S.S. - 304 IN 0.01 N DCl - D_2O SOLUTION AT DIFFERENT TEMPERATURES.

Table XV. Statistical values of exchange current densities, i_o, and Tafel slopes, b, for stainless steel at different temperatures in 0.01 N $HCl-H_2O$ and 0.01 N $DCl-D_2O$ solutions

Solution	0.01 N $HCl-H_2O$		0.01 N $DCl-D_2O$	
Temperature, °C	i_o, amps/cm^2	b	i_o, amps/cm^2	b
15	0.8500×10^{-7}	0.06346	2.940×10^{-8}	0.05528
25	1.101×10^{-7}	0.06103	4.348×10^{-8}	0.06377
35	1.695×10^{-7}	0.06206	5.545×10^{-8}	0.06424
45	2.399×10^{-7}	0.0663	10.0×10^{-8}	0.06364
55	2.800×10^{-7}	0.07833		

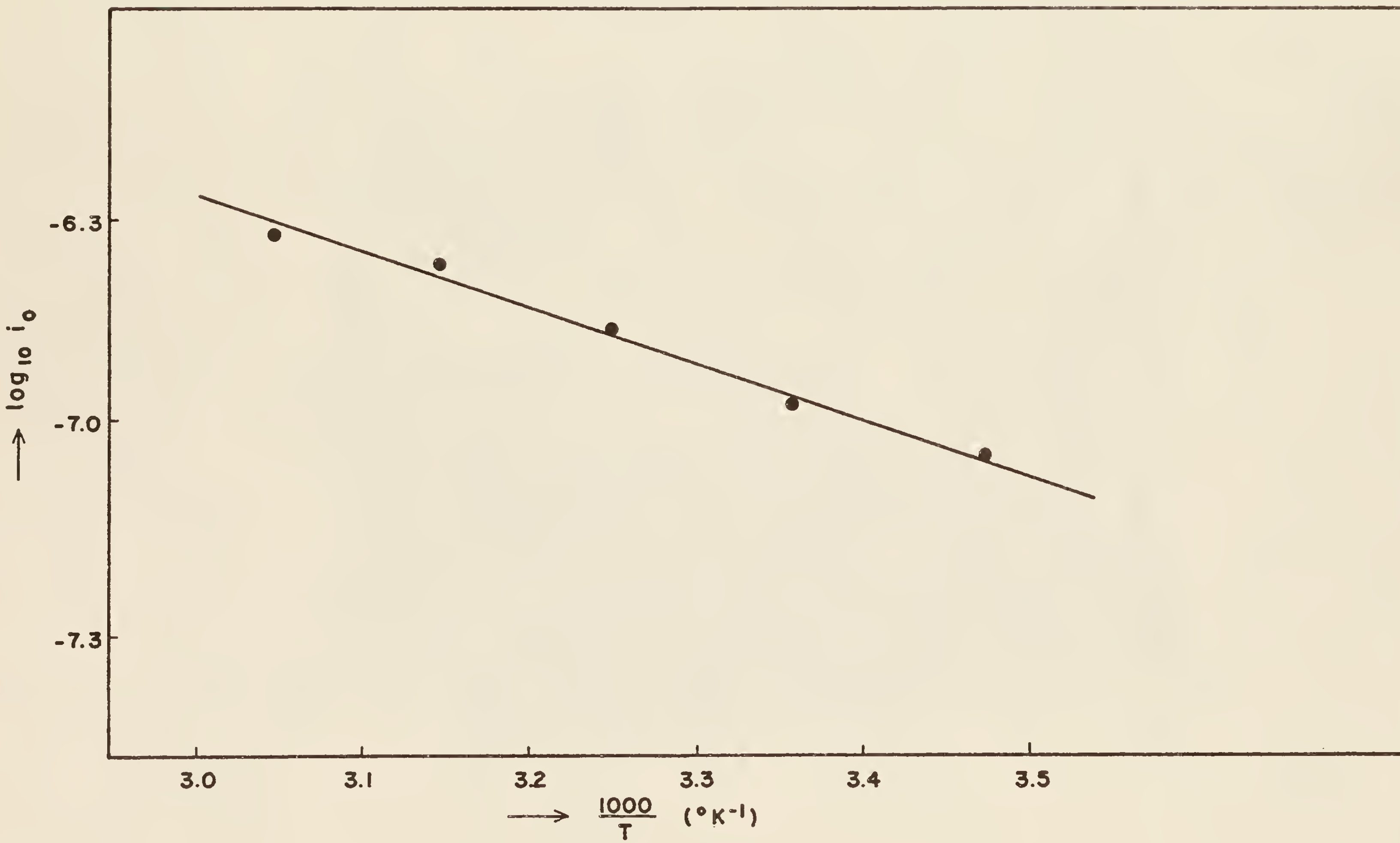

Fig. 19 RELATIONSHIP BETWEEN $\log_{10} i_o$ AND 1/T FOR S.S.-304 IN 0.01 N HCl-H_2O SOLUTION

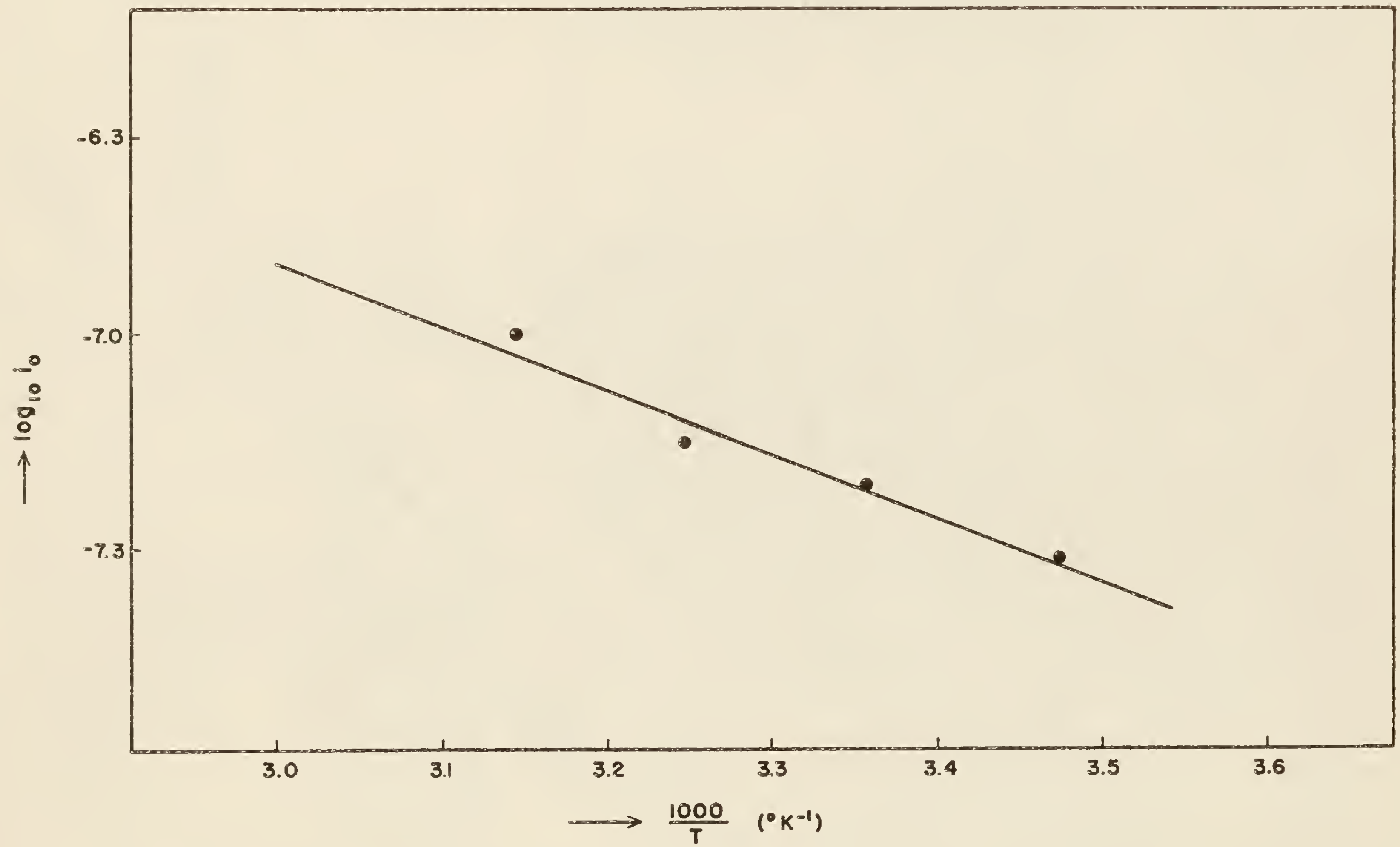

Fig. 20 RELATIONSHIP BETWEEN $\log_{10} i_0$ AND $1/T$ FOR S.S.-304 IN 0.01 N $DCl-D_2O$ SOLUTION

Table XVI. Standard heats of activations in 0.01 N $HCl-H_2O$ and 0.01 N $DCl-D_2O$ solutions

Solution	Normality	B	Least Square Slope	$\Delta H^*_{H/D}$ Kcal/mole	$\Delta\Delta H^*_{D-H}$ Kcal/mole
$HCl-H_2O$	0.01	2.73×10^{-3}	-1.30	-5.95	1.13
$DCl-D_2O$	0.01	6.72×10^{-3}	-1.55	-7.08	

Table XVII. Isotopic ratio, R, of exchange currents for Nickel

Solution	Normality	Temperature	i_o, amps/cm^2	b	$R = \frac{(i_o)H_3O^+}{(i_o)D_3O^+}$
$HCl-H_2O$	0.01	25°C	2.645×10^{-7}	0.0439	3.11
$DCl-D_2O$	0.01	25°C	8.502×10^{-8}	0.04895	

and the difference in heats of activation, $\Delta\Delta H^*_{D-H}$. Substituting this value in Eq. (183) gives limiting separation factor, S, to be 6.8. Comparing this value of S with the theoretical values recorded in Table IV shows that the rate determining step in hydrogen/deuterium evolution reaction is a simple discharge mechanism. It should be noted that in determination of ΔH^*_D or ΔH^*_H using Eq. (184), the difference in zero point energy of the hydrogen/deuterium activated states was assumed to be zero. For estimation of the magnitude of isotopic differences of zero point energies in the activated states for proton or deuteron transfer, we can regard these states as being electrostatically intermediate between the ions (H_3O^+ or D_3O^+) and the resulting neutral molecules (H_2O and D_2O). For analogous vibrational modes, the frequencies in the ion are lower than those in the corresponding molecule (48). It is assumed that the difference of zero point energy of the non-dissociating bonds, between the initial and activated states, is approximately β times the difference between the zero point energies of initial and final states where β, the symmetry factor, is equal to 1/2. Based on these considerations the relative rates of hydrogen and deuterium production by simple discharge can hence be lowered by a factor of exp[630/591], (44), i.e., 2.8 at 25°C, compared with the values previously estimated for simple discharge reaction. Hence the actual value of $S = \frac{6.8}{2.8} = 2.43$ which is in excellent agreement with the experimental value of R = 2.54.

4.3 Conclusion

Based on the experimental results and discussions presented above, the following conclusions are presented.

1. The Tafel parameters and the isotopic ratio, R, (Table XVII) obtained experimentally for Ni in 0.01 N $HCl-H_2O$ and 0.01 N $DCl-D_2O$ solutions agree within experimental error with the corresponding values reported by other investigators.

2. The average value of the Tafel slope, b, for stainless steel electrodes in 0.01 N $HCl-H_2O$ solution found to be 0.06103 indicated that the rate determining step for the hydrogen evolution reaction on stainless steel is simple discharge. It further indicated that the rate determining step for the hydrogen/deuterium evolution reaction on Cr is either simple discharge or electrochemical desorption.

3. Both the logarithm of the exchange current density and the overpotential for stainless steel in $HCl-H_2O$ solutions are linearly dependent on the pH, the slopes of these lines being -0.871 and -0.115 respectively.

4. Values of the Tafel slope b do not change with change in pH indicating that the reaction mechanism is independent of the acidity of the solution.

5. Values of the stoichiometric number, μ, ranged from 0.84 to 2.12. Comparison between these values and the corresponding theoretical values did not lead to any definite conclusions as to the rate determining step in the reaction mechanism. Other investigators (43, 47, 49) have been faced with the same difficulty.

6. Values of b for stainless steel in 0.01 N $HCl-H_2O$ and 0.01 N $DCl-D_2O$ were, within the experimental error, the same, indicating that there was no change in the rate determining step of the reaction mechanism due to deuterium substitution.

7. The isotopic ratio, R, was determined to be 2.54. This value confirmed that the overall rate determining step in hydrogen/deuterium evolution reaction on both stainless steel and Cr is simple discharge.

8. The idea of surface coverage has been found useful in correlating the experimental and theoretical values of R.

9. Tafel slopes did not change with the change in temperature both in $HCl-H_2O$ and $DCl-D_2O$ solutions for stainless steel indicating that the rate determining step is independent of temperature.

10. $\Delta\Delta H^{*}_{D-H}$ determined from overpotential measurements in $HCl-H_2O$ and $DCl-D_2O$ at different temperatures indicated simple discharge as the rate determining step in the overall reaction mechanism on stainless steel.

5.0 FURTHER INVESTIGATION

Results obtained in this work if combined with anodic overpotential studies would lead (as indicated in Section 2.5) to the determination of corrosion rates of stainless steel, thus avoiding the tedious and time consuming conventional way of determination of rates of corrosion.

Comparison of the results obtained in this study with those of identical studies on irradiated electrodes would help reveal the effects of radiation on corrosion mechanisms.

Similar studies on other alloys and on their individual constituents would help in clarifying the effect of alloying on the electrochemical behavior of elements.

6.0 ACKNOWLEDGEMENTS

The author wishes to express his deep gratitude to Dr. S. Z. Mikhail under whose direction this study has been accomplished. Sincere appreciation is extended to Dr. W. R. Kimel, Head, Department of Nuclear Engineering at Kansas State University, for his advice and encouragement. Thanks are also extended to the Department of Nuclear Engineering of the Kansas State University Engineering Experiment Station and to the United States Agency for International Development "AID" for their financial support.

7.0 LITERATURE CITED

1. U. S. Atomic Energy Commission
   Atomic Energy Facts
   U. S. Government Printing Office 1957

2. Henry, H. H.
   Materials for Nuclear Power Reactors
   Reinhold Publishing Corporation, New York 1955

3. Breden, C. R.
   Water Chemistry and Corrosion, Vol. II
   Argonne National Laboratory (Feb. 1963)

4. Uhlig, H. H.
   Corrosion and Corrosion Control
   John Wiley & Sons, Inc., New York (March 1964)

5. Stern, M.
   The Electrochemical Behavior, Including Hydrogen Overvoltage, of Iron in Acid Environments
   J. Elec. Chem. Soc., Nov. 1955, 102; 609-616

6. Stern, M.
   The Relation Between Pitting Corrosion and the Ferrous-Ferric Oxidation Reduction Kinetics on Passive Surfaces
   J. Elec. Chem. Soc., Oct. 1957, 104; 600-606

7. Bockris, J., Pentland, N., Sheldon, E.
   Hydrogen Evolution Reaction on Copper, Gold, Molybdenum, Palladium, Rhodium, and Iron
   J. Elec. Chem. Soc., March 1957, 104; 182-194

8. James, F. B.
   Anodic Passivation of Steel in 100 Percent Sulfuric Acid
   Corrosion - National Association of Corrosion Engineers, July 1963, 19; 238t-241t

9. Edeleanu, C.
   A Potentiostat Technique for Studying the Acid Resistance of Alloy Steels
   J. Iron Steel Inst., Feb. 1958; 122-132

10. Stern, M.
    The Mechanism of Passivating-Type Inhibitors
    J. Elec. Chem. Soc., Nov. 1958, 105; 638-647

11. Bockris, J., Potter, E. C.
    The Mechanism of the Cathodic Hydrogen Evolution Reaction
    J. Elec. Chem. Soc., April 1952, 99; 169-185

12. Eyring, H., Glasstone, S., Laidler, K. J.
Application of the Theory of Absolute Reaction Rates to Overvoltage
J. Chem. Phys., Nov. 1939, 7; 1053-1065

13. Glasstone, S.
Introduction to Electrochemistry
D. Van Nostrand Co, Inc., New York, July 1947

14. Glasstone, S.
The Elements of Physical Chemistry
D. Van Nostrand Co,, Inc., New York, Feb. 1961

15. Moelwyn-Hughes, E. A.
Physical Chemistry
Pergamon Press, New York, Jan. 1957

16. Glasstone, S.
Theoretical Chemistry
D. Van Nostrand Co., Inc., New York, Feb. 1961

17. Sherman, J.
Chem. Rev., 1932, 2; 93

18. Conway, B. E.
The Electrolytic Hydrogen-Deuterium Separation Factor and Reaction Mechanism
Proc. Roy. Soc. (London), 1958, A247

19. Dennison, D. M.
Rev. Mod. Phys., 1940, 12; 175

20. Born, Z.
Physik, 1920, 1; 45

21. Lange, E.
A. Elektrochem, 1938, 44; 43

22. Owen, B. B., Sweeton, F. H.
J. Am. Chem. Soc., 1933, 55; 3504

23. Lewis, G. N., Doody, F. G.
J. Amer. Chem. Soc., 1933, 55; 3504

24. Harned, H. S., Dreley, E. C.
J. Am. Chem. Soc., 1939, 61; 3113

25. Krishenbaum, J.
Physical Properties and Analysis of Heavy Water
McGraw-Hill Book Co., New York, 1951

26. Gaydon, A. G.
Dissociation Energies and Spectra of Diatomic Molecules
London: Chapman and Hall, 1953

27. Reitz, O., Forster, E.
Z. Elektrochem., 1938, 44; 45

28. Parsons, R., Bockris, J. O.
Trans. Faraday Soc., 1951, 47; 914

29. Conway, B. E., Bockris, J. O.
Modern Aspects of Electrochemistry, Chap. II
Academic Press, New York

30. Laidler, K. J.
J. Chem. Phys., 1954, 22; 1740

31. Papee, H., Canady, W., Laidler, K. J.
Can. J. Chem., 1956, 34; 1677

32. Conway, B. E., Bockris, J. O.
J. Chem. Phys., 1957, 26; 532

33. Herzberg, G.
Molecular Spectra and Molecular Structure
Van Nostrand, New York, Aug. 1959, 1; 501

34. Bigeleisen, J.
J. Phys. Chem., 1952, 56; 823

35. Bockris, J.
Modern Aspects of Electrochemistry
Butterworths Scientific Publications (London), April 1954

36, Topley, B., Eyring, H.
J. Chem. Phys., 1934, 2; 219

37. Eucken, A., Bratzler, K.
Z. Phys. Chem., 1935, 174A; 273

38. Okamoto, G., Horiuti, J., Hirota, K.
Sci. Pap. Inst. Phys. Chem. Res. Tokyo, 1936, 29; 223

39. Stern, M., Geary, A. L.
Electrochemical Polarization
J. Electrochem. Soc., 1957, 104; 56

40. Mueller, W. A.
Derivation of Anodic Dissolution Curve of Alloys from Those of Metallic Components
Corrosion Feb. 1962, Vol. 18, 73t-79t

41. Uhlig, H. H.
Z. Electrochem., 1958, 62; 700

42. Evans, U. R.
Z. Electrochem., 1952, 62; 619

43. Bockris, J., Potter, E. C.
The Mechanism of Hydrogen Evolution at Nickel Cathodes in Aqueous Solutions
J. Chem. Phys., April 1952, 20; 614-628

44. Conway, B. E.
Kinetics of Electrolytic H/D Evolution
Proc. Roy. Soc., 1960, A256; 128-144

45. Freund, E.
Mathematical Statistics
Prentice-Hall, Inc. 1962

46. Rozenthal, K. and others
Zh. Fiz. Khim., USSR, 1945, 19; 601

47. Bockris, J., Koch, D.F. A.
Comparative Rates of the Electrolytic Evolution of H_2 and D_2 on Fe, W, Pt
J. Chem. Phys., Nov. 1961, 65; 1941-1948

48. Falk, M., Giguere, P. A.
Can. J. Chem., 1957, 35; 1195

49. Azzam, A. M., Bockris, J. M., Conway, B. E., Rosenberg, H.
Some Aspects of the Measurement of Hydrogen Overpotential
Trans. Faraday Soc., 1950, 46; 918-927

APPENDIX A

Least Squares Fit for the Tafel Region and Calculation of the Stoichiometric Number from the Non-linear Region of the Overpotential Curves

The Tafel equation is

$$\eta = a + b \ln i_c . \tag{1}$$

Substituting

$$\bar{y} = \bar{\eta} \tag{2}$$

$$\bar{x} = \overline{\ln i_c} \tag{3}$$

$$y = a + bx . \tag{4}$$

The deviation is $E_i = y_i - (a + bx)$. (5)

Therefore, $(E_i)^2 = [y_i - (a + bx_i)]^2$ (6)

and $\Sigma(E_i)^2 = \sum_{i=1}^{n} [y_i - (a + bx_i)]^2$. (7)

By minimizing with respect to a

$$\frac{\delta\Sigma(E_i)^2}{\delta a} = \Sigma[-2(y_i - (a + bx_i)] = 0$$

or

$$= -2\Sigma[y_i - (a + bx_i)] = 0 \tag{8}$$

and with respect to b

$$\frac{\delta\Sigma(E_i)^2}{\delta b} = \Sigma[2(y_i - (a + bx_i)(-x_i))] = 0$$

$$= -2\Sigma[(y_i - (a + bx_i))x_i] = 0 \tag{9}$$

Therefore, rewriting equations (8) and (9) and equating to zero,

$$-\Sigma y_i + na + b\,\Sigma\, x_i = 0$$

or

$$\eta a + (\Sigma x_i)b = \Sigma y_i \tag{10}$$

Therefore, $$-\Sigma y_i x_i + a\Sigma x_i + b\Sigma x_i^2 = 0$$

or $$(\Sigma x_i)a + (\Sigma x_i^2)b = \Sigma y_i x_i. \qquad (11)$$

Solving equations (10) and (11) by Cramer's rule

$$b = \frac{n\Sigma y_i x_i - \Sigma x_i \Sigma y_i}{n\Sigma x_i^2 - (\Sigma x_i)^2} \qquad (12)$$

$$a = \frac{\Sigma x_i \Sigma y_i x_i - \Sigma y_i \Sigma x_i^2}{n\Sigma x_i^2 - (\Sigma x_i)^2} \qquad (13)$$

IBM-1410 Program for Least Squares Fit for the Tafel Region and Calculation of the Stoichiometric Number from the Non-linear Region of the Overpotential Curves

```
      MON$$     JOB TAFEL LEAST SQUARE SLOPE
      MON$$     COMT 5,3 PAGES, SHIV N KAUL,MASTERS THESIS
      MON$$     ASGN MJB,12
      MON$$     ASGN MGO,16
      MON$$     MODE GO,TEST
      MON$$     EXEQ FORTRAN,,,,,,,TAFEL
       DIMENSION AMP(40),ETA(40),EAMP(40)
     1 FORMAT(F6.2,3I3)
     2 FORMAT(E8.2,F12.6)
     3 FORMAT(5H AMP=,E14.4,5H ETA=,F12.6,18H NON-LINEAR SLOPE=,E16.8)
     4 FORMAT(4HKPH=,F6.2,4H  A=,E14.8,18H  ERROR PER POINT=,E14.8)
     5 FORMAT(1HL,20X,10HDATA SET  ,I3)
     6 FORMAT(5H AMP=,E14.4,5H ETA=,F12.6,9H DELTA E=,F12.8)
     7 FORMAT(11HKINTERCEPT=,E14.8,28H  LINEAR LEAST SQUARE SLOPE=,E18.8)
   100 READ(1,1) PH,NP1,NP,NSET
       IF(NP.EQ.0) CALL EXIT
C      NP1 IS NUMBER OF POINTS IN NON-LINEAR REGION
C      NP IS TOTAL NUMBER OF POINTS
       WRITE (3,5)NSET
       READ (1,2) (AMP(I),ETA(I),I=1,NP)
C     CONVERT INPUT ETA TO NEGATIVE VALUE
       DO 70 I=1,NP
    70 ETA(I)=-ETA(I)
C      CALCULATE DELTA E
```

```
      DO 50 I=1,NP
      DELE=ETA(I)+.059*PH
   50 WRITE (3,6) AMP(I),ETA(I),DELE
C     CALCULATE SLOPE IN NON-LINEAR REGION
      DO 20 I=1,NP1
      SLOPE=(ETA(I+1)-ETA(I))/(AMP(I+1)-AMP(I))
   20 WRITE (3,3) AMP(I),ETA(I),SLOPE
C     E PREFIX DENOTES QUANTITY IN LOGRITHMIC DOMAIN
      NP11=NP1+1
      DO 30 I=NP11,NP
   30 EAMP(I)=ALOG(AMP(I))
      NPL=NP-NP1
C     NPL IS NUMBER OF POINTS IN LINEAR REGION
C     CALL SUBROUTINE TO PERFORM LEAST SQUARE ANALYSIS
      CALL LSTSQ1(ETA,EAMP,NP11,NP,EAO,ESLOPE)
      SLOP=1./ESLOPE
      A=SLOP*EAO
      AO=EXP(EAO)
C     CALCULATE TOTAL POSITIVE ERROR PER POINT IN LINEAR REGION
      ERR=0.
      DO 40 I=NP11,NP
   40 ERR=ERR+ABS(ESLOPE*ETA(I)+EAO-EAMP(I))
      ANPL=NPL
      ERR=ERR/ANPL
      WRITE (3,4) PH,A,ERR
      WRITE (3,7)AO,SLOP
      GO TO 100
      END
     MON$$     EXEQ FORTRAN,,,,,,,LSTSQ1
      SUBROUTINE LSTSQ1(X,Y,K1,K2,AO,A1)
      DIMENSION X(40),Y(40)
      C12=0.
      C1K=0.
      C22=0.
      C2K=0.
      DO 10 I=K1,K2
      C12=C12+X(I)
      C1K=C1K+Y(I)
      C22=C22+X(I)**2
   10 C2K=C2K+X(I)*Y(I)
      C21=C12
      C11=K2-K1+1
      D=C11*C22-C12*C21
      AO=(C1K*C22-C2K*C12)/D
      A1=(C2K*C11-C1K*C21)/D
      RETURN
      END
     MON$$     EXEQ LINKLOAD
               CALL TAFEL
     MON$$     EXEQ TAFEL,MJB
```

APPENDIX B

Chemical Analysis of the Stainless Steel Sample Used for Preparation of Stainless Steel Electrodes

Name of the supplier:	American Steel and Wire Division of United States Steel Corporation	
Description of Material:	USS10-8 Type 304 Stainless Steel Wire BRT ANLD Gray Matte Finish	
Diameter:	1/16"	
Analysis:	Carbon	.08%
	Manganese	.94
	Phosphorus	.029
	Sulphur	.018
	Silicon	.53
	Nickel	8.76
	Chromium	18.76

APPENDIX C

Report on the Spectroscopically Pure Nickel Sample Used for Preparation of Nickel Electrodes

Name of the supplier: Johnson, Matthey & Co., Limited, London

Description of Material: Nickel sheet, 1/16" (The material has been prepared in special Chemicals and Metals Laboratory and of a high degree of purity.)

Spectrographic Examination: A spectrographic examination was made by means of a constant current D.C. arc, taking 5.6 amps., between pure graphite electrodes. Weighed quantities of the sample were arced in thin-walled anode cups against a horizontal machined electrode as the cathode, both electrodes being water-cooled.

Spectra were photographed simultaneously on an Ilford Long Range Spectrum plate with a Medium Spectrograph and an Ilford Ordinary plate with a Littrow Spectrograph covering the wavelength range 2200-3700A in two exposures.

Estimates of the quantities of impurities present were made by visual comparison of the spectra with those of synthetic standards, arced in a manner similar to that used in the test.

Element		Estimate of Quantity Present parts per million
Iron		8
Silicon		8
Aluminum		5
Copper		5
Calcium		2
Magnesium		2
Manganese Silver	each element less than	1

The following elements were specifically sought but not detected, i.e. either they are not present or they are below the limits of detection by the described examination procedure: As, Au, B, Ba, Bi, Cd, Co, Cr, Cs, Ga, Ge, Hf, Hg, In, Ir, K, Li, Mo, Na, Nb, Os, P, Pb, Pd, Pt, Rb, Re, Rh, Ru, Sb, Se, Sn, Sr, Ta, Te, Ti, Tl, V, W, Zn, Zr.

During fabrication some surface contamination is unavoidable and for this reason the samples used for this spectrographic analysis have been pickled in hot dilute nitric acid before examination.

APPENDIX D

Calculation of the Difference in the Isotopic Heats of Activation from Potential Energy Diagrams

The initial and final state potential energy curves for H and D are shown in figure (21):

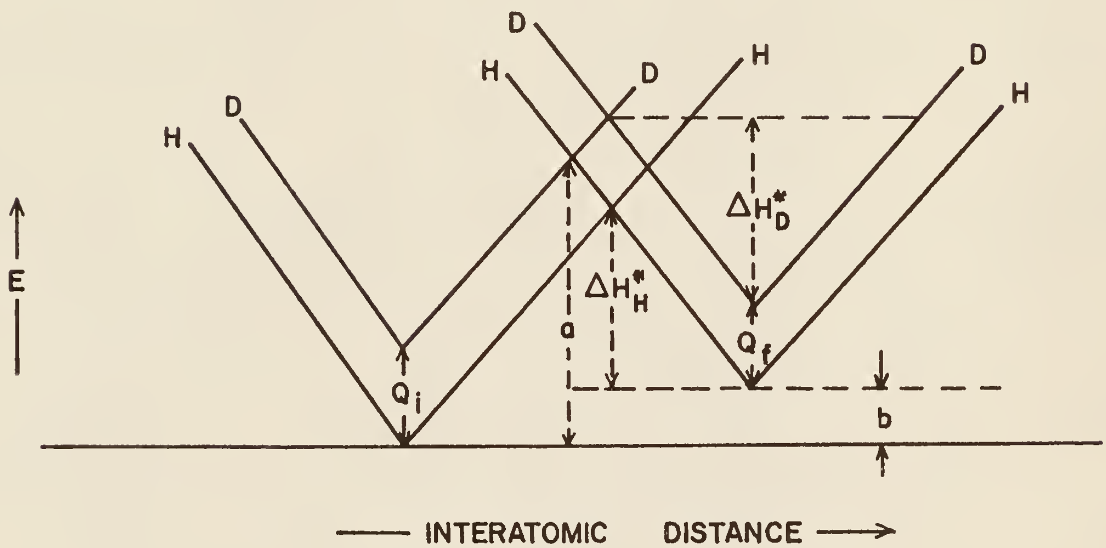

Fig. (21) Potential Energy Diagram

Neglecting the zero point energy differences of the initial state, the following geometric relationships can be obtained from the above figure.

$$\Delta H_H^* = a-b-\beta Q_i$$

$$\Delta H_D^* = a-b+\beta Q_f-Q_f$$

$$= a-b-(1-\beta)Q_f$$

where β is the symmetry factor and Q_i and Q_f are the differences between the minima of the potential energy curves of hydrogen and deuterium species for the initial and final states, respectively.

Thus $\Delta H_D^* - \Delta H_H^* = \beta Q_i - (1 - \beta)Q_f$

and if $\beta = 1/2$, $\Delta H_D^* - \Delta H_H^* = 1/2(Q_i - Q_f) = 1/2\ \Delta Q$

Now, correcting for the zero point energies of the initial state, the required activation energies are

$$\Delta H_{o,H}^* = \Delta H_H^* - (z.p.e.)_H$$

$$\Delta H_{o,D}^* = \Delta H_D^* - (z.p.e.)_D$$

or $$\Delta H_{o,D}^* - \Delta H_{o,H}^* = 1/2\ \Delta Q + (z.p.e.)_H - (z.p.e.)_D$$

where z.p.e. = zero point energy.

EFFECT OF SUBSTITUTION OF DEUTERIUM FOR HYDROGEN IN WATER ON THE ELECTROCHEMICAL KINETICS OF STAINLESS STEEL-304

by

SHIV NATH KAUL

B. S. (Chem. Engg.) BANARAS HINDU UNIVERSITY, INDIA, 1957

AN ABSTRACT OF
A MASTER'S THESIS

submitted in partial fulfillment of the

requirements for the degree

MASTER OF SCIENCE

Department of Nuclear Engineering

KANSAS STATE UNIVERSITY

Manhattan, Kansas

1965

ABSTRACT

The purpose of this work was to study the electrode kinetics of hydrogen evolution on stainless steel-304, to determine the effect of deuterium substitution on the reaction mechanism and to evaluate the hydrogen-deuterium separation factor on stainless steel-304, a factor of extreme importance in the electrolytic production of heavy water. The reaction mechanisms were studied by conducting cathodic polarization runs on stainless steel-304 electrodes in ultra-purified systems of 0.01 N $HCl-H_2O$ and 0.01 N $DCl-D_2O$. Comparison between the experimental values of Tafel parameters and their corresponding theoretical values led to determination of the rate determining step of hydrogen/deuterium evolution reactions. The separation factor, S, was evaluated both by determining the isotopic ratio, R, of exchange current densities in light and heavy water and by determining the isotopic difference in heats of activation from overpotential measurements carried out at different temperatures in light and heavy water. The value of S evaluated from the isotopic ratio was 2.5 ± 0.9 and the value of S based on heats of activation was 2.4 ± an estimated standard deviation of 0.9.

Cathodic polarization measurements were also taken by using nickel electrodes in the same solutions. The Tafel parameters and isotopic ratio, R, agreed with those reported by other investigators.

The values of Tafel slopes obtained in the light and heavy water systems were in agreement within experimental error and both values characterized the overall rate determining step in the hydrogen/deuterium evolution reaction as simple discharge. The stoichiometric number, μ, was determined from the slopes of the non-linear region of the Tafel curve in the light water system.

The isotopic ratio, R, was found to be equal to 2.5 $\pm$ 0.9. Comparison of this value with the corresponding values obtained from thermodynamic considerations confirmed that the rate determining step in hydrogen/deuterium evolution reaction is simple discharge.

Based on the above values of S and R it was shown that the rate determining step of the hydrogen/deuterium evolution reaction on chromium was also that of simple discharge. This method made it possible to study such elements as chromium which otherwise cannot be studied independently because of their high reactivity.